NASW-4435

NASA-CR-195550

NASA/USRA OSU 3

THE OHIO STATE UNIVERSITY

IN-07-CR

204271

P. 60

Abstract

According to Aviation Week and Space Technology(November 16, 1992), "without a redefined approach to the problem of achieving single stage-to-orbit flight, the X-30 program is virtually assured of cancellation." One of the significant design goals of the X-30 program is to achieve single stage to low-earth orbit using airbreathing propulsion systems. In an attempt to avoid cancellation, the NASP program has decided to design a test vehicle to achieve these goals. This report will recommend a conceptual design unmanned test vehicle using airbreathing propulsion system.

Executive Summary

This report will examine the feasibility of achieving single stage-to-orbit flight. It will analyze the integration of a scramjet propulsion system into a waverider lifting-body configuration. It will show in depth the trajectory characteristics, aerodynamics, propulsion systems, and weight and volumes. It will also provide supporting information of landing gear, thermal protection system, and cost breakdown.

Table of Contents

		Page
Introduction		1
Aerodynamics	Chapter1	2
Design Methodology		3
Vehicle Performance		5
Trajectory	Chapter 2	5
Propulsion	Chapter 3	8
Weight	Chapter 4	14
Volume Analysis		16
Landing Gear		17
Thermal Protection Systems		21
Aircraft Cost Analysis		24

List of Figures

Figure		Page
1.	Conic Flow-Exact 3-D Solution	28
2.	Minimum Length Moc Nozzle	29
3.	Airez Model	30
4.	L/D vs Mach #	31
5.	Cl vs Alpha	32
6.	Drag Polar	33
7.	Cdo Components	34
8.	Free Body Diagram Of Flight Vehicle	35
9.	Mach # vs Altitude	36
10.	Mach vs Altitude	37
11.	Time vs Weight	38
12.	Range vs Altitude	39
13.	Map Course	40
14.	Time vs Altitude	41
15.	SFC for different types of engines	9
16.	Performance Cycle For Different Prop. Systems	9
17.	Performance Comparison of Fuel	42
18.	Ramjet Engine Schematics	43
19.	Ramjet Engine Temperature	44
20.	Scramjet Engine Schematics	45
21.	Scramjet Engine Temperature	46
21b.	Thrust and Ramdrad vs Mach #	12
22.	Thrust vs Mach #	13
23.	Weight Pie Chart	47

24. Volume Pie Chart 48

25. Skid Landing Gear Schematic 49

25b. Temperature Distribution 50

26. Forebody Configuration 51

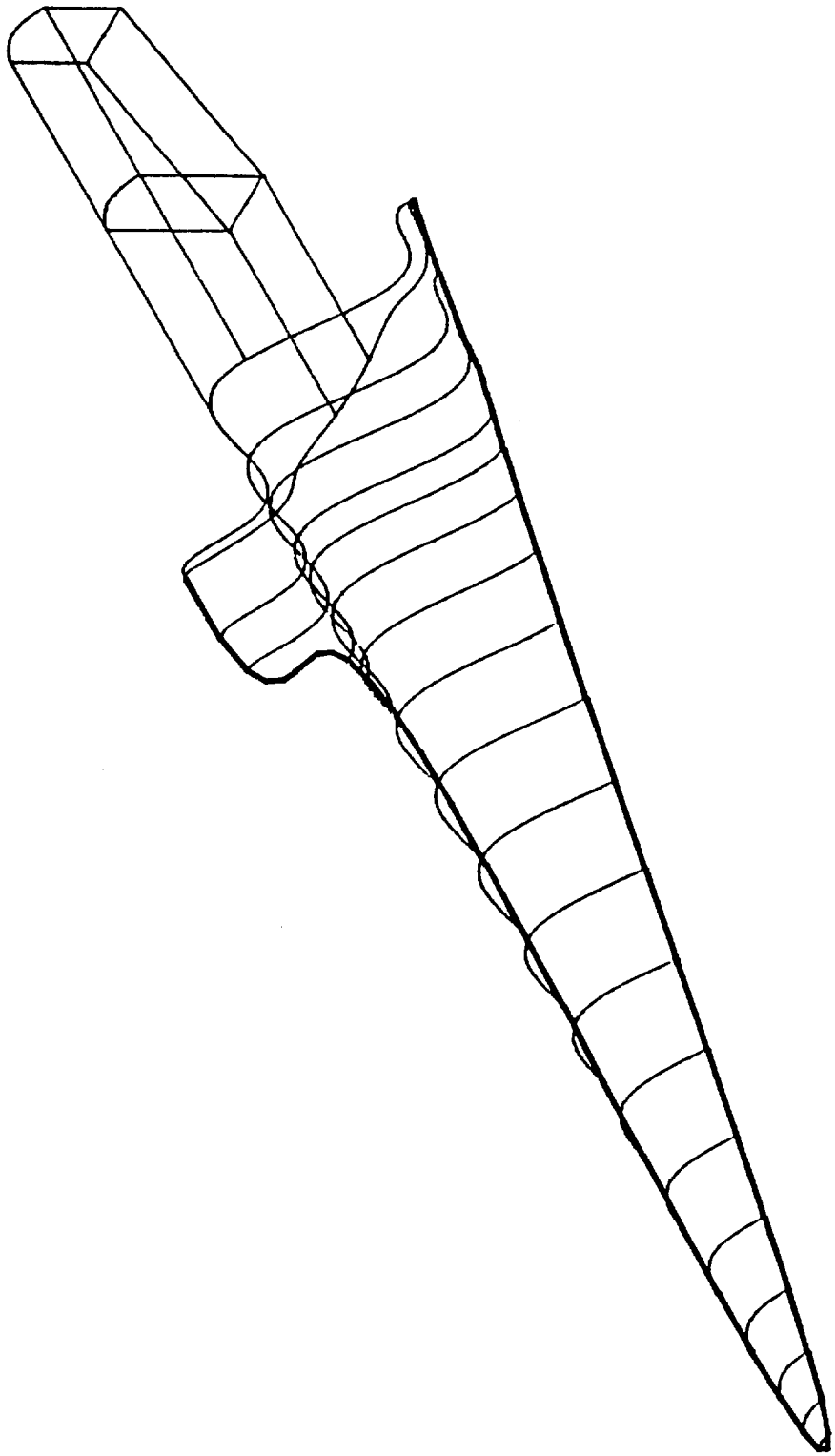

EXPERIMENTAL HYPERSONIC TEST VEHICLE

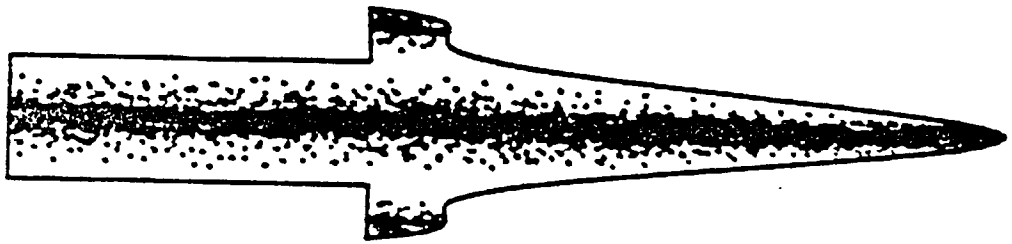

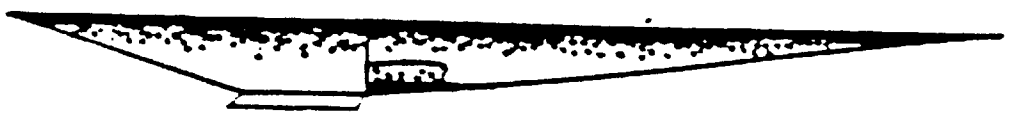

Introduction

Since the 1960's, NASA and other government agencies have tried to produce a single stage-to-orbit vehicle that only uses air breathing engines. When the National Aerospace Plane (NASP) project began, the effort became a pure research endeavor. The major driving factor supporting the continuation of this project was to reduce the space launch cost to about one hundredth of the current costs.

Within the last two years, the NASP project has suffered budget cuts and cost over runs. Now facing discontinuation, NASP officials have decided to reassess the need for the project. As a result of several meetings, NASP officials want to test fly a hypersonic vehicle for two reasons. The first reason is to determine whethre or not hypersonic flight is attainable with current technology and the second reason is to help redefine the problem of single stage-to-orbit flight.

IN January, 1993, NASA in conjunction with The Ohio State University asked a senior design group to design a conceptual hypersonic test vehicle that can achieve a low earth orbit subject to a specified mission profile. The Details of this mission are in the following section.

MISSION PROFILE

The mission of team GRAY III is to design an unmanned hypersonic test vehicle which will be launched from a carrier aircraft designed by a team from Ecole Polytechnique Feminine. The vehicle is to test an airbreathing propulsion system and take data on boundary layer transition at a flight condition between mach 12 to 15, and 100k to 120k ft altitude. The test duration is one minute at steady conditions, and the vehicle must accommodate 1000 lbs. and 35 cu.ft. of test equipment.

Initially, the vehicle was to be launched at mach .8 and 40k ft. Later in the design process, the designers of the carrier aircraft decided that a mach 2, 50k ft. launch was

feasible. This allowed a massive scale-down of the test vehicle. This scaled down version will be presented in this paper.

AERODYNAMICS

The first major decision of the aerodynamic group was to choosing a configuration. There are three basic types of configuration: wing-body, lifting body, and waverider. A realistic aircraft will probably take concepts from each of these configurations, but a careful trade study will give a place to start as well as insight into what modifications might be made.

The wing-body configuration is aptly named, consisting of a delta wing and cylinderical body. One of its several advantages is high volumetric efficiency. The entire volume of a cylinder is easily utilized. This simple geometry, along with the relatively flat, squared-off lifting and control surfaces make this configuration the least costly to manufacture. The design and analysis of this configuration is also made easier due to plentiful experimental flight data available for study. Despite these benefits, the fatal characteristic of this configuration is the lift-to-drag ratio in the hypersonic regime. The propulsion systems under consideration will have much difficulty providing the thrust required for the flight conditions.

The lifting-body configuration is a vehicle with a body design driven by aerodynamic considerations. Like the wing-body, this configuration tends to have an excellent volumetric efficiency. The lift-to-drag ratios of the lifting body are much better in the hypersonic regime. The aerodynamic shape of the lifting-body, however, makes it expensive to manufacture.

The waverider configuration is designed using the exact 3-D solution of a conical flow. One characteristic of this design is that the shock at the design point is attached to the entire leading edge. This results in the best lift-to-drag ratio of all considered

configurations. The complex geometry of the waverider makes it expensive to manufacture. Waveriders are also an untested concept.

The configuration chosen for this study is the waverider. Since the test vehicle is to be launched in the supersonic regime and will not have to propel itself through the sonic pinch, less fuel is needed and volume restrictions are alleviated. Expense of manufacture will be much the same for lifting-bodies and waveriders. The propulsion system may be easily integrated into the waverider shape. Although this is a virtually untried concept, the small vehicle size and short mission makes this an ideal oppurtunity to test a waverider.

DESIGN METHODOLOGY

The body and propulsion system of a hypersonic aircraft must be highly integrated. This is because the shocks generated by the body will have a significant effect on the propulsion system and there is great potential for interference. Additionally, a given parcel of fluid passes from nose to tail so quickly that any compression process must begin at the nose and expansion must continue to the tail for efficiency. The body of the GRAY III aircraft is entirely determined by the SCRAMJET engine and the design point conditions.

The waverider forebody of the aircraft is designed using a methodology developed by Rasmussen. A sixth degree function, using only even powers, is arbitrarily chosen for the free-stream trailing edge of the body. The function describes a curve at a non-dimensionalized distance from the tip of the shock-generating cone. A line through each point on the curve and parallel to the lengthwise axis, may be traced forward until it intersects the shock cone. The surface described by this set of lines is the free-stream surface of the waverider, and the locus of points where these lines intersect the shock cone is the leading edge. From the leading edge, the known streamlines of the conical shock

flow are traced back to the axial position of the base, describing the compression surface. These streamlines bend away from the cone axis and the free-stream surface, creating a volume. (see fig. 1)

Rasmussen's method for generating a waverider body was chosen for the great control over geometry that this method allows. By varying coefficients of the free-stream trailing edge function, the volumetric efficiency and some aerodynamic characteristics may be affected. A function was chosen for the GRAY III vehicle that gives reflexed winglets and an easily usable cross-section.

As noted above, the forebody shape is determined almost completely by the engine inlet requirements. Varying the angle of the shock generating cone will vary conditions behind the shock. This cone angle is chosen based on the conditions required at the engine inlet. The geometry is scaled such that the engine inlet covers the greatest possible area bounded by the waverider compression surface and the circular arc of the shock.

The aft part of the aircraft consists of a minimum length, two-dimensional, one-sided nozzle designed by method-of-characteristics. At the exhaust plane, there is a sharp corner which is the origin of a centered Prandtl-Meyer expansion fan. The fan is divided into several characteristic lines radiating out to a surface parallel to the exhaust flow, and reflected back to describe the nozzle geometry. The geometry is such that the characteristics are not reflected again from the nozzle surface. The geometry of the nozzle is non-dimensionalized to the throat heighth and may be scaled to the engine size. (see fig.2)

For a full expansion, the nozzle is prohibitively long and must be truncated. In fact, for the length limitations and engine used in the GRAY III aircraft, the nozzle is truncated before the first characteristic line is reflected back to the nozzle surface. This means that the nozzle may be quite simply designed by merely calculating the initial turning angle at the throat and extending this line to the desired length.

VEHICLE PERFORMANCE

The off-design analysis of the GRAY III aircraft was accomplished using AIREZ, a code which uses a combination of wing-body theory, DATCOM methods, and empirical data.

The vehicle aero model uses a cylindrical body of equivalent total volume and equivalent length to the waverider. The nose of the model is a cone with an angle equivalent to the waverider shock generating cone angle. The nose is cambered upwards such that the tip lies at the upper edge of the cylinder. The model wing is in two parts, the first being a rectangle of the approximate span and chord of the winglets. Strakes are added to give an equivalent planform area. (see fig. 3) Output from AIREZ is displayed in figs. 4-7.

At the writing of this paper, a program is under development to calculate wave drag using area rule, and skin friction drag using flat plate approximations. This data will be used to compare with the AIREZ data in hopes that redundant results will be obtained.

TRAJECTORY

The mission profile for the OSU3 waverider begins at Mach 2 and 50,000 feet. A carrier aircraft being developed by a French team of aeronautical students will airdrop the vehicle at this prescribed velocity and height. The OSU3 aircraft will then propel itself to the test altitude and velocity of Mach 13.5 and 106,000 feet. The test phase will consist of a one minute cruise at the test altitude. The engines will shut down after the one minute test and the aircraft will return to the ground in an unpowered glide. The landing will take place on the dry lakebeds of Edwards Air Force Base in southern California.

The aircraft OSU3 uses all airbreathing propulsion. One ramjet is used from Mach 2 to Mach 6, and one scramjet is used the rest of the way. The vehicle is unmanned and Atherefore g-loadings and heating problems are not as large a priority. The trajectory program ETO was developed at the Wright Research Development Center at Wright-Patterson AFB. This is a two-degree-of-freedom program which used five equations of motion describing velocity, flight path angle, weight, altitude, and range of a hypersonic vehicle. The first diagram shows the free body diagram of a flight vehicle (see Fig. 8). The thrust required can be found from

(1) Trequired = (Wi / (L/D)max i) + mtotal (dv/dt)i

The thrust required will decrease as altitude is gained. The weight is decreasing at the same time as fuel is spent.

The trajectory used for the hypersonic test vehicle approximates the Energy Method and trades altitude for speed in the beginning. A constant Q trajectory is used for the majority of the climb. The dynamic pressure (Q) used was 2300 lb./ft.2 As the aircraft nears the test altitude, the flight path angle decreases and the aircraft was commanded to a one minute cruise and Mach 13.5. The Mach versus Altitude graph (see Fig. 9) shows the ascent phase. The altitude trade off is clearly shown on the left. The full trajectory is depicted in the second graph (see Fig. 10). The descent phase begins at the end of the one minute cruise. The power is cut and the thrust becomes zero. A commanded flight path angle is utilized during the descent. The angle of attack is maintained at 5 degrees through the whole glide portion. A small flight path angle was used until the plane reaches a low Mach number at a high altitude. The angle was then decreased (negative angle) to reach the ground and land at a reasonable speed.

The time versus weight graph (see Fig. 11) shows the decrease in the weight as the flight progresses. The initial weight is 14,261 lb. The consumption of fuel is the only loss in mass in flight. The fuel is generally used as a propellant, but some fuel is used to cool the plane. Liquid hydrogen used for cooling the vehicle is then pumped into the engines.

The descent phase also requires hydrogen for cooling, but the engines will be off and the hydrogen will be recirculated through the system. The final landing weight is approximately 11,400 lb.

The range (see Fig. 12) is plotted against the altitude with the major objective being to determine the launch and landing points. Since this is a two stage vehicle, the French aircraft will carry the test vehicle out to the launch point at the maximum range. The landing point has been determined to be Edwards Air Force Base since it can handle experimental aircraft.

The test vehicle will be dropped at 50,000 feet above the Pacific Ocean at the maximum range. Flying over the Pacific Ocean will allow the vehicle to avoid populated areas. This is an important consideration when dealing with an unmanned, experimental aircraft. The map course (see Fig. 13) shows the planned route of the aircraft.

The time versus altitude plot (see Fig. 14) shows the flight duration. The aircraft requires about 500 seconds to climb to the test altitude. The cruise phase lasts sixty seconds and then the power is shut off. The descent phase lasts approximately 600 seconds.

Further work is needed with the descent phase. There are many different methods, such as constant angle of attack, constant Q, and constant g-load to name a few. Each method has a different time of descent and range. A shorter range may be desired if the carrier aircraft is not capable of transporting the test vehicle the distance required. A landing phase study through the subsonic region is an important area of consideration. The characteristics of the vehicle at subsonic speeds is not known and the plane may have trouble making a controlled landing.

Follow-up work is required on what has been accomplished thus far. Other programs should be used in order to compare results. Optimization is also a project goal and low costs. All of these need to be considered as research continues on this type of system.

PROPULSION

The design of a propulsion system, as in any other system, involves certain restrictions and limitations; also there are many directions that can be followed and trade-offs to be made according to the mission requirement.

Just as a quick reminder, our mission requires a one minute flight test at mach 12-15 and at 100000 to 130000 ft altitude. Our vehicule will be dropped by the french vehicule at mach 2.2 at 51000 ft. Our goal is to use airbreathing system from the dropoff point until the test altitude(106000 ft).

This kind of flight is possible through two types of systems: the first system would be a combination of Rocket/Scramjet engines, and the second system would be a combination of Ramjet/Scramjet engines. But since using a rocket would add more complications to the system(more fuel and weight), the ramjet/scramjet combination seemed more attractive and challanging option. This system has better performance and more efficient than the other system.

Figure 15 shows that the specific fuel consumption for rocket engine is 10 times higher than that of the air breathing engines. Also figure16 (ISP vs Mach number) indicates that the rocket performance is the lowest among other types of engines.

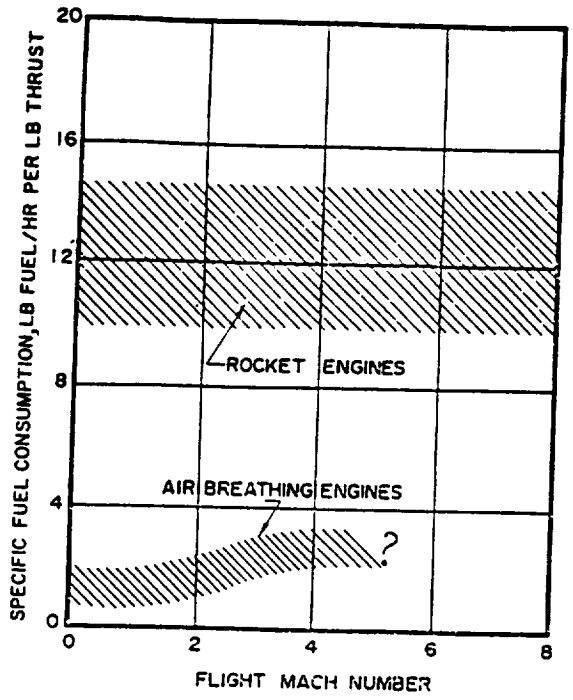

Figure 15: specific fuel consumption for different type of engines

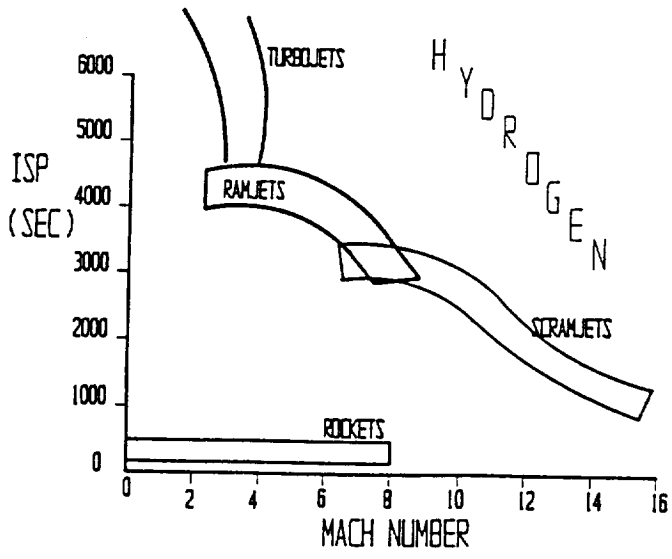

Figure 16: peformance cycle for different propulsion systems

The operation of the ramjet depends on two factors : flight mach number and type fuel used. From a mechanical view point, the ramjet is the simplest of all air-breathing jet engines. Although the ramjet engine can be designed to operate at subsonic flight speeds, the nozzle expansion ratio P5/P04 is too small to give a high thermal efficiency. The higher the flight mach munber at a given altitude, the larger the cycle pressure ratio P02/P2 and the more efficient is the ramjet engine. For flight mach above approximately M= 3 has a level fuel consumption rate then any gas-turbine jet engine. If the ramjet engine is to operate over a wide range flight mach numbers a variable area inlet and a variable area exhaust nozzle- which complicates the engine and increases its weight, are required.

Since our goal would require the ramjet engine to operate from Mach 2.2 - 7, a fuel comparison was necessary. Figure 17 shows a performance comparison for JP4, Methane, and Hydrogen at Mach 6.0; hydrogen is the most efficient for our mission; although its low density is a disadvantage because it contributes to large volume "large airplane". However, as it will be discussed later in the weight and volume section, 39% of the vehicle volume is empty. A schematic of the ramjet engine is shown in Figure 18; the static temperature throughout the engine are shown in Figure 19; the maximum static temperature is at the combustor exit (4300 R).

When the stagnation temperature at station 4 (T4) exceeds approximately 5000 R there may be significant dissociation of the combustion products and the result of injecting more fuel may cause further dissociation instead of an increase in T4. At flight mach numbers exceeding approximately Mo=7.0 the stagnation pressure recovery of the diffusion system decreases rapidly due to the strong shocks, and the static temperature of the air entering the burner becomes too high for obtaining satisfactory ramjet engine. The static temperature can become so high that no heat release can be achieved in the burner.

The basic disadvantage of the ramjet and scramjet engines is that the nozzle pressure ratio P4/P5 depends entirely upon the flight mach number and the performance of the diffusion system. Consequently, a ramjet can not develop static thrust.

The difficulties which limit the operating flight mach number of ramjet engines arise primarily from the necessity of decelerating the induced air to approximately M2=0.2 at the entrance of the burner so that satisfactory combustion of the fuel can be achieved in a subsonic stream of air. The scramjet removes the limitations described above; scramjet engines can be operated at a wide range of mach numbers with fixed geometry. More over, its internal pressure and temperature at the entrance of the burner will not be excessive since the diffused flow is supersonic throughout. Figure 19 shows a schematic of a scramjet engine that would be intergrated into an airframe [Based on NASA TM-X2895 by John R. Henry and G. Y. Anderson of NASA Langley (A73)].

Deleting edge of the cowl was made coincident with the engine throat in order to starting capability. Fuel is injected perpendicularly and parallel to the air stream from the side plates and the strut through orifices. Injection conditions are sonic for normal injection and supersonic for parallel injection, the later being contributing to thrust and for avoiding undesirable expansion of the mainstream due to the step. Diameters of normal injection orifices are 1.0 mm and those for parallel injection at the throat are 1.5 mm on the side plates and 2.1 mm on the strut, both with expansion area ratio of 4.0 mm. The difference in diameters of parallel injection orifices between the side plates and the struts is due to the fact the strut must feed just twice the amount of fuel fed from the side plates.

As a major material, a copper alloy utilized in the combustion chamber of LE-7 liquid hydrogen rocket engine under development for F-II launch vehicle of Japan is adopted. This material was shown to have sufficient strength at high temperature with

high thermal conductivity. Cooling water passages are channel structure with rectangular cross-section, which is based on experiences on the cooling technology of rocket engine combustion chamber. The static temperature throughout the scramjet engine are shown in Figure 20; a maximum static temperature of 5100 R is at the combustor exit. As for the ramjet, the net thrust increases as the flight mach number increases at a given altitude; however, as we increase the air flow rate and the mach number, we are adding a certain amount of energy to the system and getting little or nothing back because of heigth dissociations; this means that the ramdrag increases proportionally with the gross thrust, the result is a small increase in the net thrust.

$$Fn = Fg - Ramdrag$$

The engine performance is shown in Figure 21

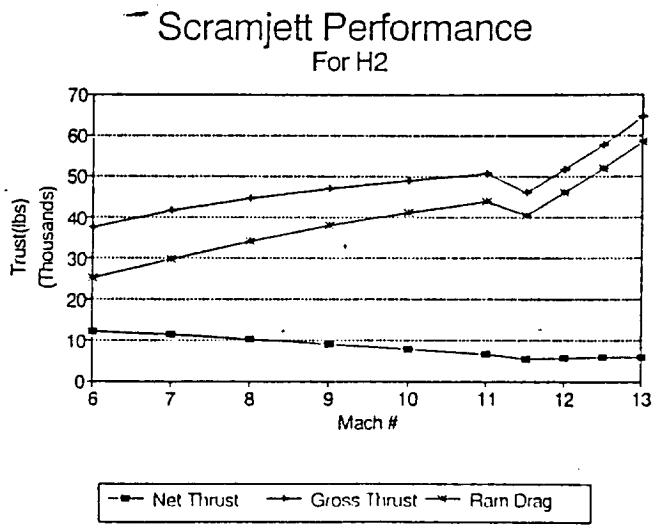

Figure 21; thrust and ramdrag versus mach number plot for scramjet

Engine specification and performances are shown in Table p-1. These performance data correspond to the flight trajectory requirements. The net thrust and thrust required vs. mach number for the trajetory up to the end of the test phase is shown in Figure 22. A maximum thrust required of about 18,000 lbs. occurs at mach 4.5 and then the thrust decreases as the mach number and the altitude increase.

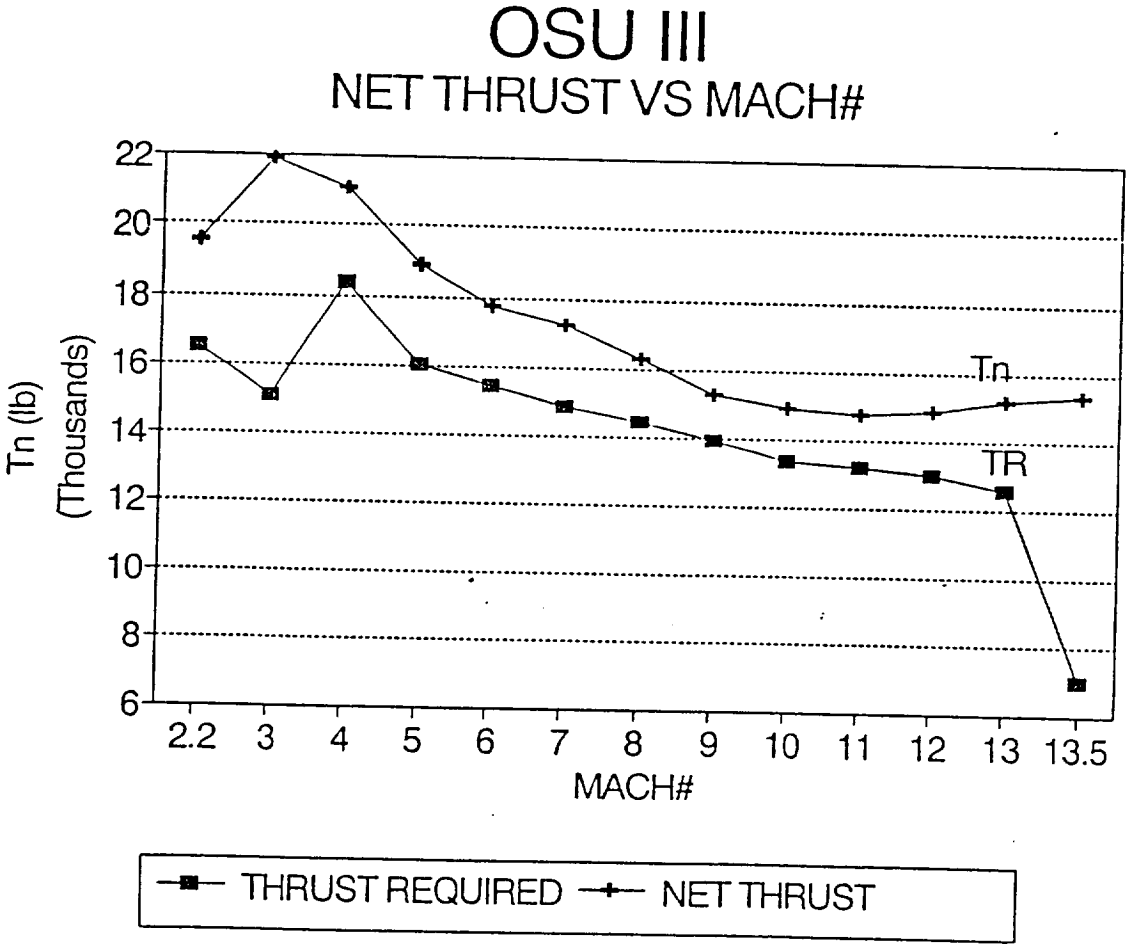

Figure 22: Thrust vs Mach No. plot

ENGINE SPECIFICATIONS AND PERFORMANCES

	RAMJET	SCRAMJET
WEIGHT (LBS)	1520	1260
LENGTH (INCHES)	150	136
WIDTH	36	36
HEIGTH	24	26
MACH NO.	2.2-7.0	7.0-13.5
ALTITUDE (FEET)	51000-77000	77000-106000
SFC (LBM/HR/LBF)	.99-1.8	1.4-2.6
MAX. ISP (SEC)	3624	2594

Table 1

At test altitude where the vehicle is no longer accelerating the thrust required drops to about 6500 lbs. and the net thrust increases as we reach the cruise altitude because the speed is still increasing without changing altitude and as is stated before the thrust increases with mach number and decreases with altitude.

The next section will discuss weight and volume.

WEIGHT

The weight of the aircraft was determined from the computer program PDWAP. This program is based on the weight analysis program WAATS developed for NASA in the 1970's. Empirical formulas for different components were developed base on existing airframes. PDWAP initially sizes and figures the needs of an aircraft based on several inputs. A data file is created which is then used as the input for the weight analysis section. The created data file can be edited to customize the data for a known dimension

or component weight. The data file can then be resubmitted to the weights analysis section for new weights.

A weight pie chart (see Fig. 23) shows the percentage of the total weight each component weighs. The fuel compromises 24.6% of the total launch weight. The 1000 lb. payload consists of 7.0% of the total. The launch weight of the system is 14,261 lb. and the landing weight is about 11,400 lb. The landing weight depicted below is lower since the program does not consider that some of the propellent will be used only for cooling. There is around 600 lb. of hydrogen that will not be used to propel the vehicle. Due to evaporation, there will be a loss in the extra hydrogen carried that is not accounted for in the trajectory.

Below is a detailed breakdown of the weights.

Number of RamJets = 1 Thrust per eng.: = 20,000 lbs.
Fuel = 3,510 lbs. Fuel Density = 4.400

Weights:

GTOW = 14,261 lbs.
Entry = 10,748 lbs.
Landing = 10,741 lbs.
Dry = 9,732 lbs.
Payload = 1,000 lbs.

Weight Statement (all measurements in lbs)

==========

Group 1: Body structure= 4,591
Basic body= 2,446
Secondary= 764 Thrust= 194 Integral fuel tanks= 1,187 Integral Ox tanks= 0

Group 2: Thermal Protection System= 948
Cover panels= 0
Vehicle insulation= 948.

Group 3: Launch and Recovery Gear= 356
Launch gear= 36
Landing gear= 320

Group 4: Propulsion= 2,076
Rocket engines= 0
Turboramjet= 0 Ramjets= 1,080
Nonstructural fuel tank= 0 Nonstructural Ox tank= 0 Fuel tank insulation= 350 Ox tank insulation= 0 Fuel system= 177 Oxidizer system= 0 Pressurization system= 359 Inlets= 70

Group 5: Orientation Control System= 473
Engine gimbal system= 0
Attitude control system= 167 Aerodynamic controls= 263 Seperation system= 43
ACS tankage= 0

Group 6: Power supply= 398

Electrical System= 376 Hydraulic/Pneumatic Sys= 22
Group 9: Avionics= 889

Vehicle Dry Weight= 9,732
Group 10: Payload= 1,000
Group 11: Residual Propellant= 9
Trapped fuel= 9
Trapped Oxidizer= 0
Landing Weight= 10,741
Group 12: Reserve Propellants= 7
Fuel= 7
Oxidizer= 0
ACS fuel= 0
ACS oxidizer= 0

Entry Weight= 10,748
Group 13: Inflight Losses= 4
Fuel= 4
Oxidizer= 0
Group 14: Main Propellants= 3,510
Fuel= 3,510
Oxidizer= 0

Gross Weight= 14,261

Volume Analysis

It is generally viewed that the volumetric efficiency of a waverider type aircraft is rather poor. Due to many thin areas of the aircraft, the actual usable volume that the aircraft provides is small. However, in the OSU III design, a waverider with a large amount of volume was developed. This was done by the incorporation of two different ideas. The first idea was the actual theoretical design process of the aircraft (Rasmussen's method) which allowed for a greater volumetric efficiency than previous designs which were examined (for instance that design which is generated by the MAXWARP waverider design and analysis program). A second, and more productive, idea was to incorporate two additional body sections into the design of the aircraft which served to increase the volume by over twice its original capacity. These two additional body sections were added on to the aircraft as a section which incorporated the exhaust nozzle of the aircraft and a section which was the area of the body onto which the engines were mounted. As a result, the following list shows the total volume and volume breakdown of the aircraft.

A pie chart analysis of the volume distribution of the aircraft may also help in visualizing the volume breakdown which is given below (see fig. 24).

Thermal Protection Systems: 67.15 ft3 (3.4%) Landing Skids : 29.63 ft3 (1.5%)

Liquid Hydrogen Fuel : 1007.20 ft3 (51.0%) Ramjet Engine : 51.35 ft3

(2.6%) Payload : 39.50 ft3 (2.0%) Unusable or Unused : 780.17 ft3

(39.5%)

Total Volume of Vehicle : 1975 ft3

After seeing this breakdown, there are a couple of points which need further explanation. As can be seen, there was volume allocated to the ramjet engine but not to the scramjet engine. The reasoning for this is that the ramjet has better performance characteristics the closer it is mounted to the bottom of the aircraft. As a result, the ramjet engine was partially incorporated into the body of the aircraft in order to keep it as close as possible to the aircraft's underbelly. At the same time, no volume was allotted to the scramjet engine because the scramjet would be mounted below the ramjet engine and would be totally outside of the body of the aircraft. A second clarifying point is the 'Unusable or Unused' portion of the volume breakdown. As was previously stated, the design of the waverider (or any aircraft for that matter) does not allow for the use of 100% of the available volume. The problem that was encountered was that it was found to be difficult to determine what fraction of the waverider would actually be usable. To compensate for this, a large block of volume was left unused. At the same time, it was felt that all of this unused volume was most likely more than enough to compensate for the aircraft's unusable volume, so this in turn represents an opportunity to downscale the aircraft to a smaller size. This procedure of downscaling will, of course, result in a smaller volume of the aircraft, a smaller weight, and a less expensive overall product.

Aircraft Recovery System

A final challenge, after the cruise phase of the aircraft's trajectory is completed, is the descent and recovery of the vehicle. The obvious and most common form of aircraft

recovery is the standard landing gear (landing struts, tires, etc..). However, even though conventional landing gear is by far the most popular means of getting an aircraft back on the ground, it is not the only means by which to complete the task. Although a complete and detailed analysis of the design (and the pros and cons) of different forms of aircraft recovery systems was not conducted, the OSU III group did an initial comparison of three different types of recovery systems. These systems were the aforementioned conventional type landing gear, a parachute type recovery system, and a non-conventional skid type landing gear.

The first type of recovery system that was looked at was a conventional landing gear. The advantages of this type of landing gear are that the gear provides for smooth and comfortable landings and relatively quick and easy care and maintenance. The disadvantages of this system are that the landing gear can become rather heavy when all of the components (actuating motors, tires, struts, shock absorption devices, etc..) are taken into account. These same components can also begin to take up more volume than is desired. For a wave-rider aircraft designed for hypersonic speeds, the volume and weight categories are particularly critical and a small savings anywhere can be extremely helpful. Another factor which has to be considered is being able to keep the landing gear cool enough so that the heat load which the gear is exposed to does not become so great as to cause damage to the components of the landing gear. This means either locating the gear in an area which is cool enough naturally (which may not be possible) or actively cooling the gear (adding more weight and taking up more volume). Since the aircraft is to be an unmanned test vehicle, the above advantages are not able to overcome the disadvantages for a conventional landing gear system and therefore this type of recovery system did not seem to be the most feasible one.

The second type of recovery system which was considered was a parachute and flotation device system. The aircraft would be brought down from the test speed to a more reasonable, probably subsonic, speed and at that point a parachute would deploy and the

aircraft would most likely be splashed down into an ocean. At this point the flotation device would be deployed to keep the aircraft from sinking until the aircraft could be retrieved from the water. The main advantage of this system seems to rest in the fact that the design of the vehicle results in rather poor handling characteristics upon landing. The advantage of a parachute system would then be that the aircraft would not have to be exposed to the landing and very low speed flight conditions. A second advantage is that by parachuting the aircraft into the ocean, the flight path of the aircraft can be designed as to keep it away from populated areas. Since this is an experimental aircraft the idea of flying it far from any population is an attractive one. However, the parachute system also has its' disadvantages. First, as with the conventional landing gear system, the parachute system is particularly sensitive to very high temperatures. It would be truly disastrous to deploy the parachute only to find that it has been melted and destroyed by the high heat values encountered in hypersonic flight! This means that the system must either be actively cooled, placed in a cool spot on the aircraft, or both. A second disadvantage is that the structure of the aircraft, especially in the vicinity where the parachute connects to the aircraft, must be reinforced in order to withstand the forces which the aircraft will encounter upon opening the parachute and "splashing down." This again results in an increase in both volume and weight necessary to employ this type of recovery system. A third disadvantage is that this type of recovery system is really twopart; once the aircraft has splashed down it must be recovered and brought back to its' land base. This most likely entails having a U.S. Navy ship deploy in order to recover the aircraft. While the cost of such an endeavor was not determined, it was assumed that it would most likely be substantial. For these reasons (cooling/location , volume/weight, and cost) it was decided that the parachute/flotation recovery system was also not the best system for the OSU III aircraft.

The final recovery system that was looked at was a nonconventional skid type landing gear (see fig. 25). Since the test aircraft is designed to be unmanned, there are

many advantages to a skid system. It was previously stated that this test aircraft would be air-launched from a carrier aircraft, which would eliminate the need to taxi and take-off from a normal runway. Because of this, the landing skids could be designed so that they would be pre-retracted into the aircraft and would be deployed in a simple "one-shot" manner upon landing. This would decrease the necessary weight and volume by eliminating additional actuating motors for retraction and deployment of the landing gear. It appears that this type of landing gear is approximately 2.5-3.0 % of the empty weight of the aircraft. For the OSU III aircraft this means a weight for the landing gear of approximately 250-300 lbs or 2.8% of the vehicle landing weight. A second advantage of this type of system is that the temperature is not as great a concern as was the case with the previous systems. Since there are no tires (for conventional landing gear) or fabric/vinyl material (for a parachute/flotation system) which have to be protected from melting, the temperatures which the landing gear can be exposed to can be considerably higher. A third advantage is that the relatively simple design of the skid gear system would prove to be rather inexpensive in cost and not a great difficulty in upkeep and maintenance. A disadvantage of this system is that upon landing, the great amount of friction force put on the skid could easily result in a high rate of deceleration. This however, is not as problematic as it could be since the test vehicle is unmanned (therefore injury to pilots due to high deceleration factors do not have to be considered). What does have to be addressed in this problem is making sure that the landing structure of the aircraft is sufficient to withstand the forces encountered upon landing.

Another disadvantage is that this type of landing system does not allow for easy maneuvering of the aircraft while it is on the ground. However, because of the circumstances of this particular mission, it is unnecessary for the aircraft to maneuver or even take off from the ground. A final problem with this type of system is that upon landing, part of the skid will be destroyed due to the very high friction forces encountered.

One proposed skid configuration was an inner core of magnesium alloy castings which are lined with steel shoes. The two layers would then be separated by some type of thermal insulator (possible plastic) in order to protect the magnesium castings. During landing, it is likely that the steel shoes would be melted and/or ground away so that the skids would have to be replaced after each flight. While there is some cost involved with this, it seems as though the cost would be relatively minimal when compared to the overall costs of the other types of recovery systems. For these reasons the skid type landing gear system was chosen as the recovery system to be employed on the OSU III test aircraft.

THERMAL PROPTECTION SYSTEMS

The hypersonic enviroment is very harsh due to the wxcessive surface temperatures that vehicles experience. The test conditions for the OSU 3 wave rider area maximum velocity of mach 13.5 at an altitude of 110,000 feet. During these conditions the aircraft's skin temperatures ranges from a high of 5856 F at the nose cone to 1800 F for the panels in teh midrear of the aircraft (see fig.25). The analysis for the temperature distribution was arrived from the following equation for heat transfer

$$Qdot = (3.21e\text{-}4)\, cf\, p\, v^3 \quad [1]$$

The skin friction coefficient is calculated from turbulent compressible flow on a flat plate. The heat transfer is then equated to radiation from the surface to form a heat balance. The following equation's results are the wall temperatures.

$$Tw = (Qdot / e / b)^{.25} \quad [2]$$

This procedure creates the temperature distribution for most of the aircraft. The areas of stagnated flow, mainly th nose and leading edge of the wing, are calculated slighlty differently using equation 3.

$$Qdot = 15 (p / R)^{0.5} (v / 1000)^{3} \cos^{1.5} del \quad [3]$$

The result is used in equation 2 to provide the wall temperatures. The result is highly dependent on the values for R, the radius of the nose or leading edges, used. While in the ideal case the nose and leading edge should be sharp (R close to zero), however to keep th temperatures in teh realistic range, a value of 1.00" was taken for the calculations. A sweep angle of 80 degrees was used for the leading edge.

Once the surface temperatures are calculated, materials that can withstand the thermal loads must be selected. A wide range of possibilites exist, but two types will be used exclusively. Carbon-carbon structure is perhaps the most advanced material that can be used. It can remain structurally intact in temperatures exceeding 6000 F. However, the atmosphere at high mach numbers will react and oxidize the carbon-carbon material, thus to be reusable it must be protectively coated. The oxidation coating is typically silicon cartbide and its nessecity limits the maximum temperatures to 3000 F, which is the limit of the coating. The carbon-carbon will consist of a woven cloth material with the carbon fibers aligned in the thickness direction, to increase the thermal conductivity of the material. The entire C-C layer should be a uniform thickness of 0.06". The carbon-carbon protected panels will be used for the first ten feet of the forebody, measured from the leading edge (see fig.26). The remainder of the aircraft will be covered with multiwalled panels. The multiwalled concept consists of several very thin (50 microns) foils of

Molybdium separated by insulating material. The result is a panel that is mechanically strong, light weight, and can handle maximum temperatures of 2375 F.

For areas in which the thermal loads exceed the limit for the carbon-carbon, another method for thermal protection is employed, active cooling. Cooling provides a conductive surface for the skin of the aircraft, thus reducing the wall temperatures through heat flow. The most logical method for active cooling is to use the crypgenic fuel (liquid hydrogen) for cooling purposes. Teh fuel most likely will be pumped directly fromteh storage tanks to hot regions (i.e. nose cone) and then the heated hydrogen will be routed to the engine for burning. Another method for active cooling is to use heat pipes. Heat pipes are designed to absorb heat from the hot sections by vaporizing a working fluid and radiating the heat by condensing the fluid in a larger, cooler region. Thermal transport devices on the wing can be arranged in two configurations, spanwise and chordwise. Chordwise heat pipes radiate the heat from stagnation points and spanwise pipes redistributes heat from possible excessive hot spots. Pipes will be made of tungsten with a 0.5" diameter and a 0.005" wall thickness. The internal fluid will be liquid lithium. The pipes will be constructed within the carbon-carbon skin.

For saftey concerns a combination of heat pipes and hydrogen cooling will be placed so as to cool the nose, leading edges, engine components, and control surfaces. Through the use of protective panells and active cooling, the aircraft should be protected from the aerodynamic heating.

Aircraft Cost Analysis

The determination of the cost for the aircraft was the final step in the hypersonic design process. Since cost is a driving factor in almost any endeavor, the lower the overall cost of the aircraft the better for the entire program. The cost of the aircraft was calculated by using a series of empirical equations developed for use in determining the cost of other experimental aircraft. These equations were then matched to existing aircraft in order to get a better estimation of the accuracy of the method. The original cost rates used in the equations were originally based on 1970 dollars and were then converted to 1986 dollars. These figures were further modified in order to get the 1986 dollars into current 1993 dollars. The cost analysis was broken down into a variety of different sub-groups: Engineering costs, Development costs, Flight test operations costs, Tooling costs, Labor costs, Quality control costs, Materials costs, and finally the cost to develop and produce the ramjets required for the mission. The following tabular breakdown shows the dollar amounts for each of these categories and finally the total cost for each aircraft and the project as a whole.

Engineering cost: $ 60,318,196.00

Development cost: $ 40,789,808.00

Flight Test Operations cost: $ 8,283,509.00 Tooling cost: $ 25,696,122.00

Labor cost: $ 50,879,228.00

Quality Control cost: $ 6,614,300.00

Materials cost: $ 1,272,271.00

Ramjet cost: $135,260,400.00

Total cost per aircraft: $139,105,456.00

Total Program Cost: $417,316,384.00

It should be noted that this projected cost will most likely increase due to a number of unknown factors. The first of these factors is that the price of the scramjet engine which

will be used on the aircraft was not included into the cost analysis because of the fact that very little was known on the projected cost of such an experimental engine type. Also, the projection of cost for the ramjet engine which will be used is also subject to much scrutiny because of much the same reasoning as was given for the scramjet engine. Another factor which was not considered was the cost of fuel needed in order to complete testing on the aircraft. It was felt however that the cost of fuel would be a rather small part of the overall cost of the aircraft. Finally, it is very possible that the cost of producing the OSU III test aircraft could be substantially more considering the unique design of the waverider concept. It is unknown if new production facilities would be required to complete construction or whether existing facilities could be modified to complete the task, however, in either case there would most likely be a substantial cost associated in producing an as yet untried waverider type aircraft.

Appendix A

Team Members

Abbas I. Abdallah	Team leader/Propulsion
Doug Sheridan	Trajectory
Kevin Kirby	Weight/Landing gear
Matthew Seto	Aerodynamics
Todd Winington	Thermal Protection System

REFERENCES

1. ETO - A Trajectory Program for Aerospace Vehicles, June 1989 (MS:Q-BASIC). (Wright-Patterson Air Force Base, OH: Aero Propulsion and Power Laboratory; Wright Research Development Center).

2. Conway, H. G. Landing Gear Design. Published by Robert Cunningham and Sons LTD. London, England, 1958.

3. Lawing, Peirce L. Analysis of Various Descent Trajectories for a Hypersonic-Cruise, Cold-Wall Research Airplane. Washington D.C.: National Aeronautics and Space Administration, NASA Technical Note, June 1975. TN D-7860.

4. Nicolai, Leland M. Fundamentals of Aircraft Design. Distributed by METS, Inc. San Jose, 1975.

5. PDWAP - Preliminary Design and Weights Analysis Program, 1989 (MS:Q-BASIC). (Wright-Patterson Air Force Base, OH: Aero Propulsion and Power Laboratory; Wright Research Development Center).

6. Ramscram, NASA Lewis Engine Code, Chris Snyder.

7. GE Engine Data, GE Aircraft Engines, Cincinnati, Ohio.

8. AIAA 89-2676, A Comparison of Scramjet Engine Performances Among Various Cycles, by T. Kanda, G. MAsuya, Y> Wakamatsu, N. Chinzei, And A. KAnmuri National Aerospace Laboratory, Japan

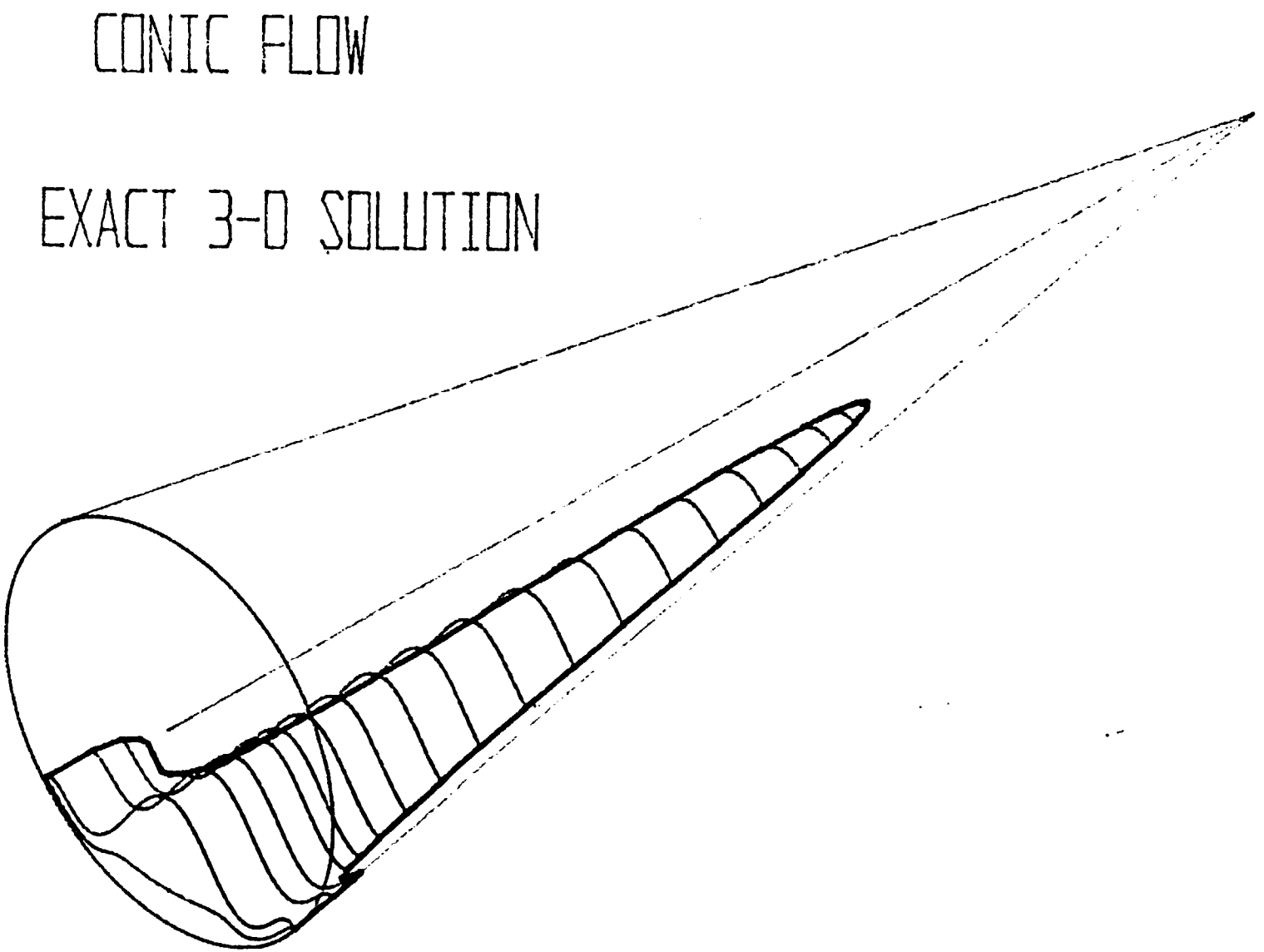

Figure 1

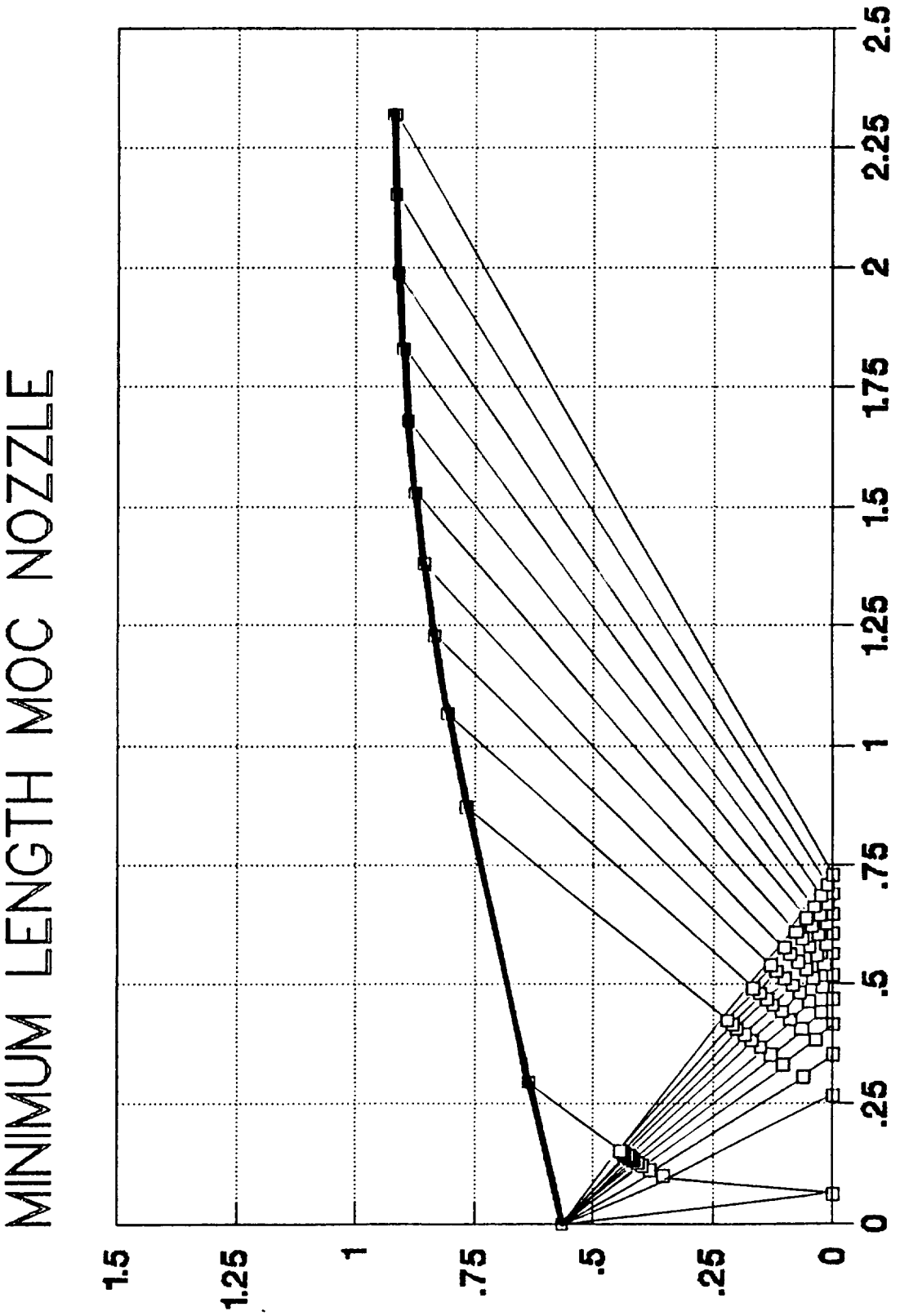
MINIMUM LENGTH MOC NOZZLE
1.5
1.25
1
.75
.5
.25
0
0
.25
.5
.75
1
1.25
1.5
1.75
2
2.25
2.5

Figure 2

AIREZ MODEL

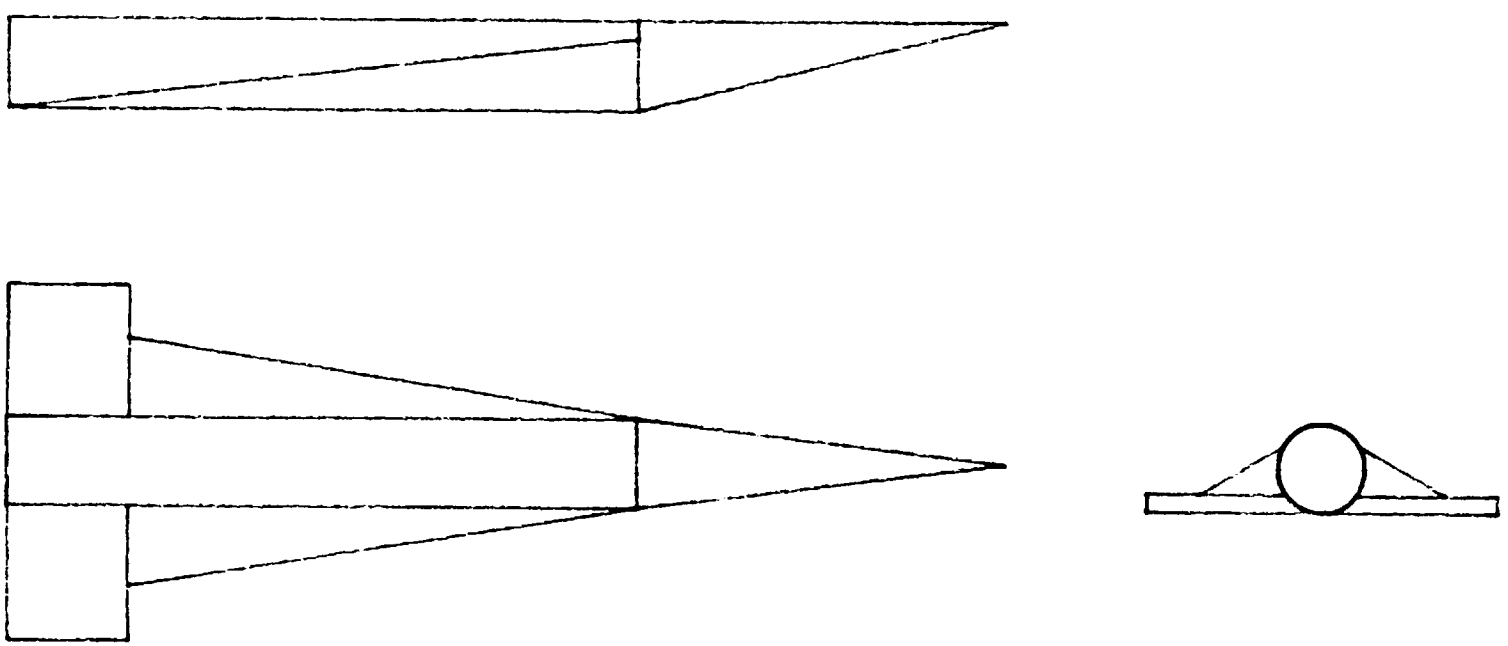

Figure 3

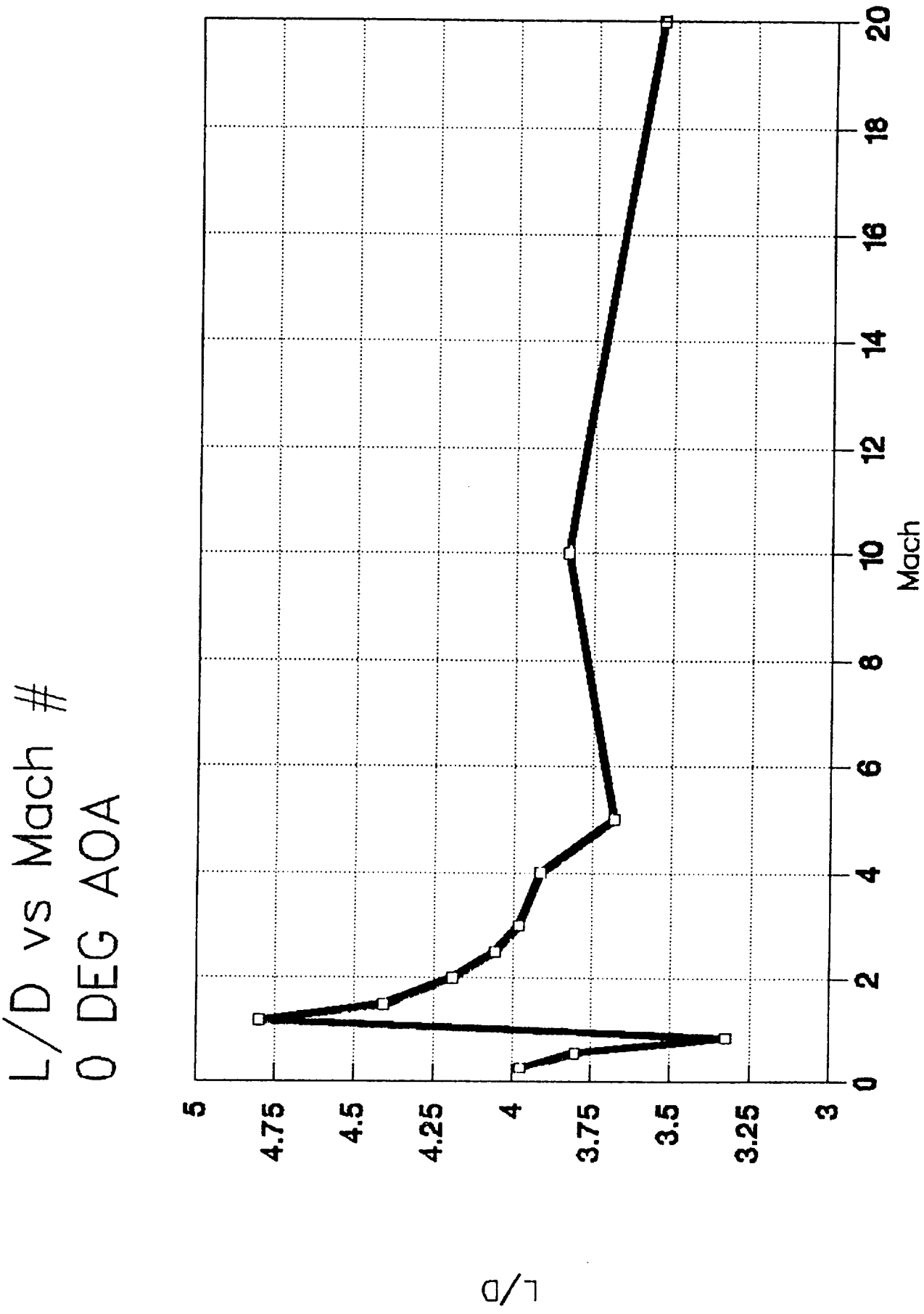
L/D vs Mach #
0 DEG AOA
L/D
5
4.75
4.5
4.25
4
3.75
3.5
3.25
3
0
2
4
6
8
10
12
14
16
18
20
Mach

Figure 4

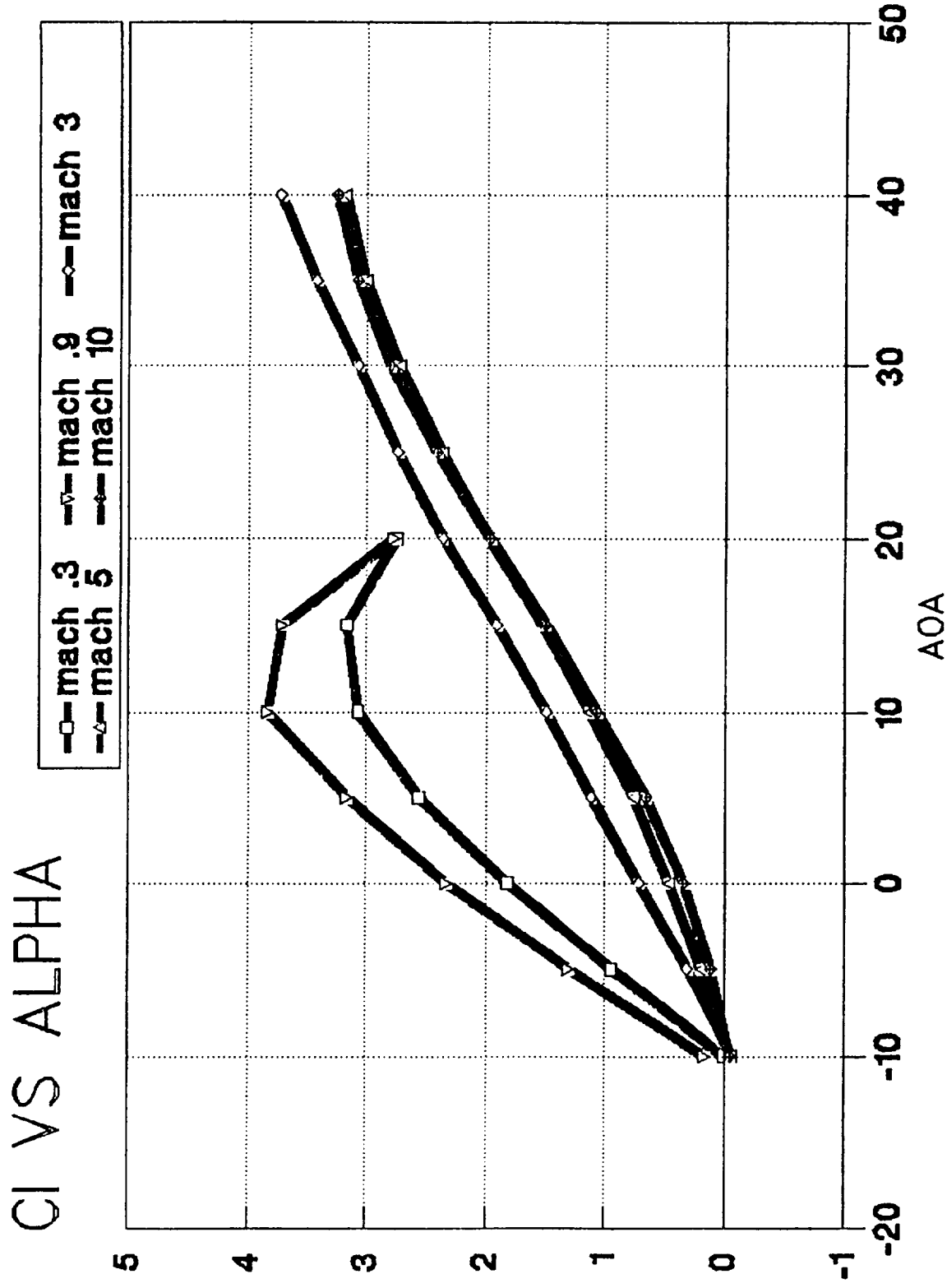
CL VS ALPHA
mach .3
mach .5
mach .9
mach 10
mach 3
CL
AOA
5
4
3
2
1
0
-1
-20
-10
0
10
20
30
40
50

Figure 5

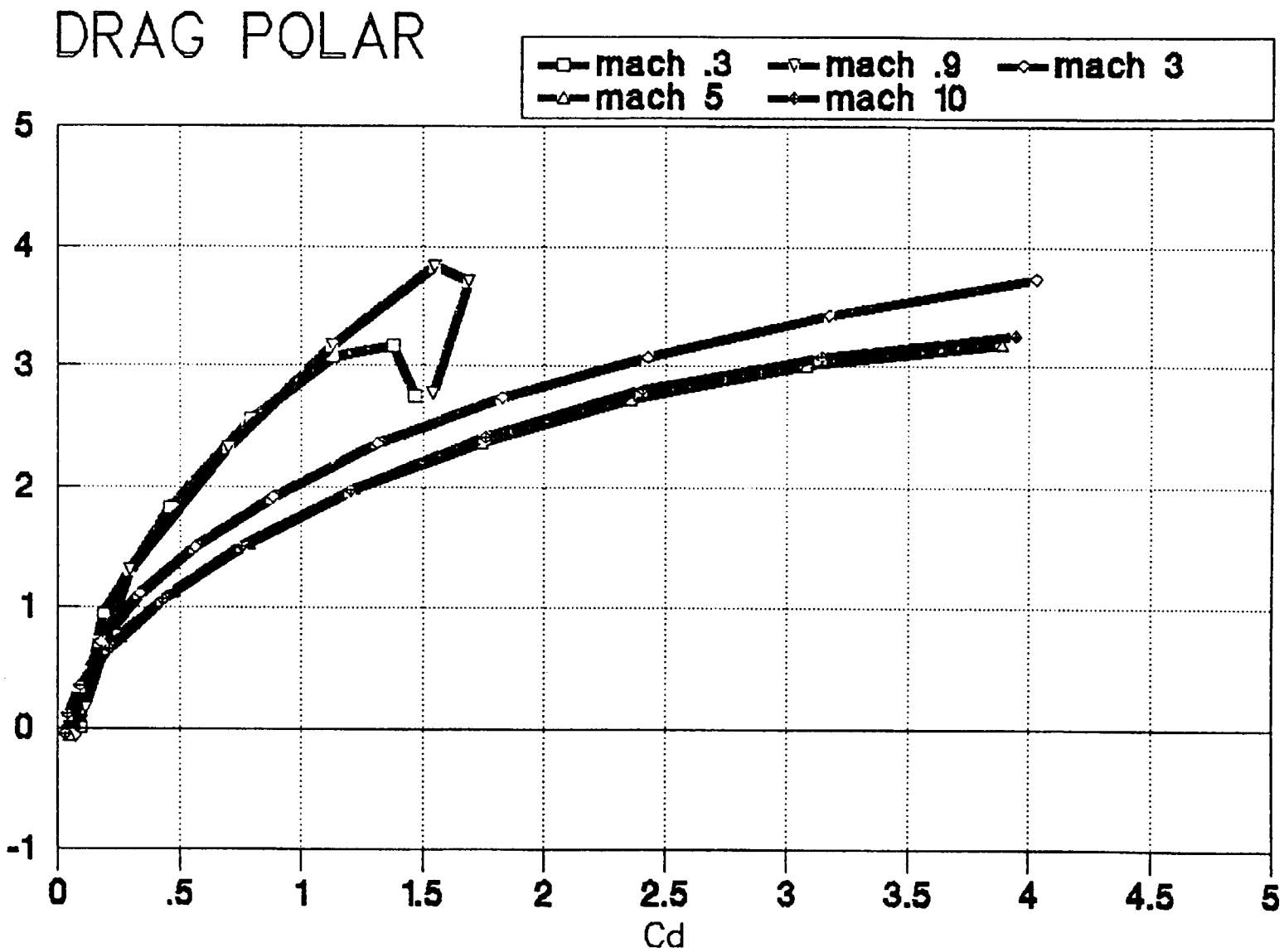
DRAG POLAR
mach .3
mach .9
mach 3
mach 5
mach 10
5
4
3
2
1
0
-1
0
.5
1
1.5
2
2.5
3
3.5
4
4.5
5
Cd
Cl

Figure 6

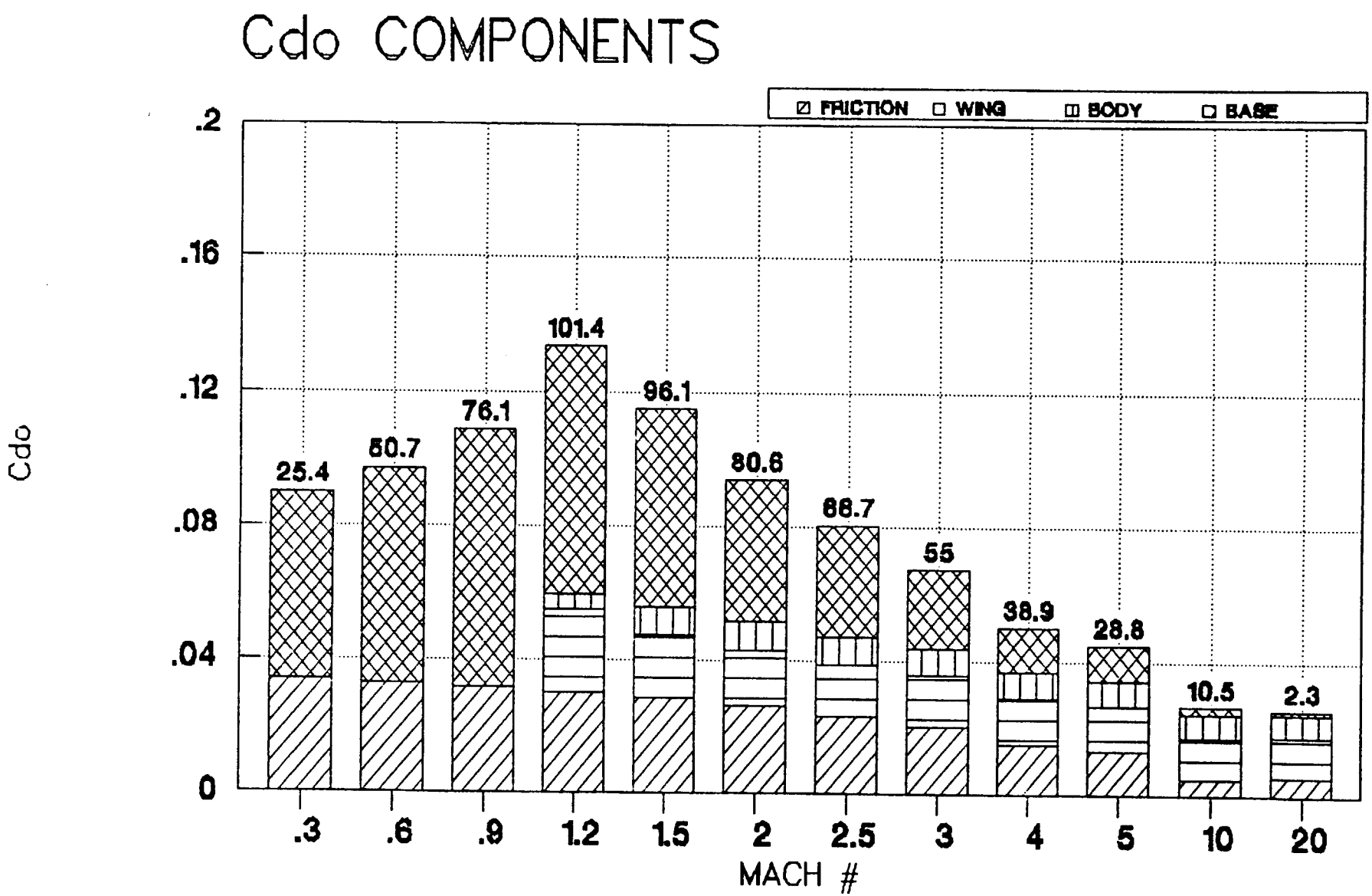
Cdo COMPONENTS
FRICTION
WING
BODY
BASE
Cdo
.2
.16
.12
.08
.04
0
25.4
50.7
76.1
101.4
96.1
80.6
66.7
55
38.9
28.8
10.5
2.3
.3
.6
.9
1.2
1.5
2
2.5
3
4
5
10
20
MACH #

Figure 7

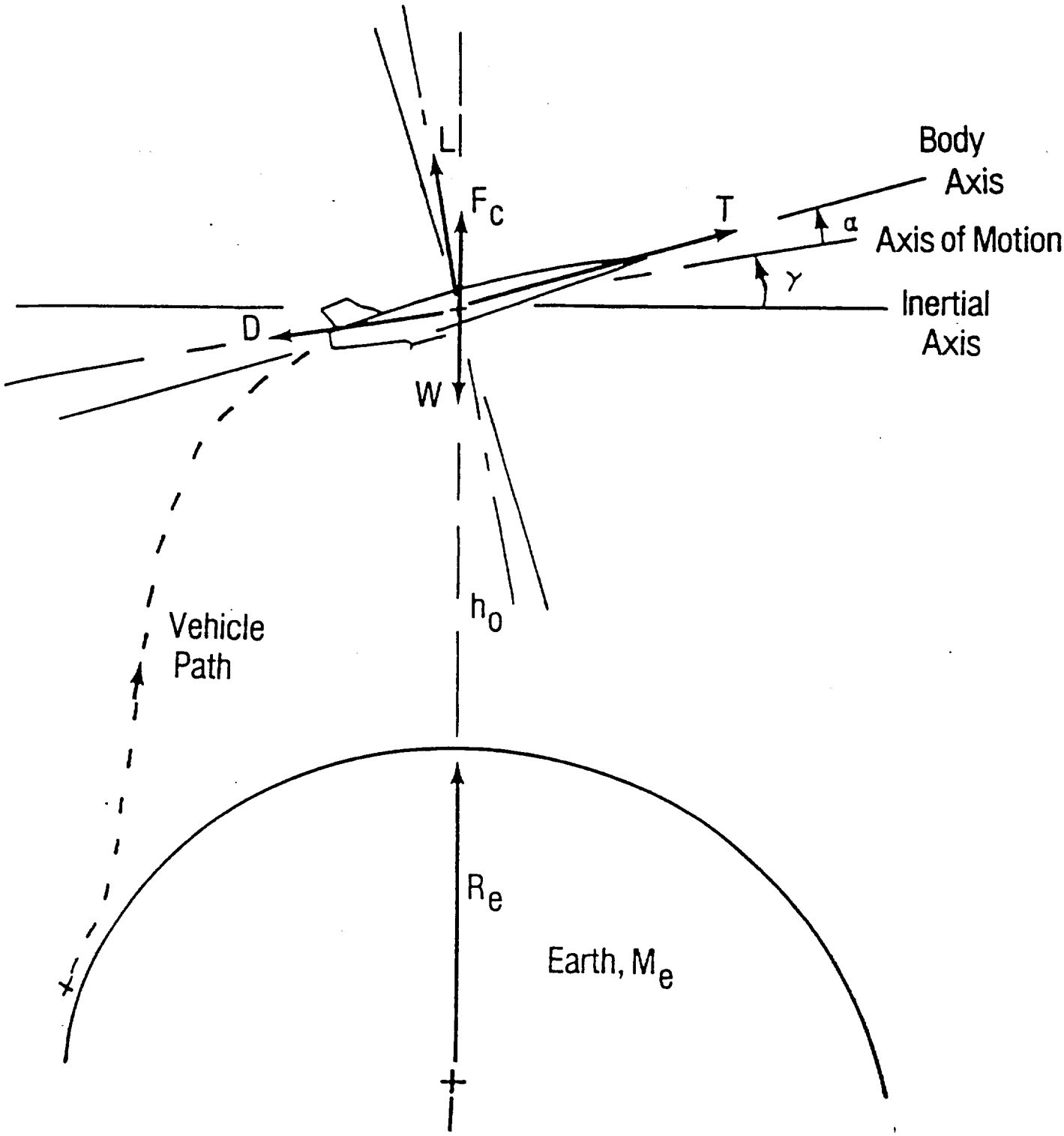

Figure 8 Free Body Diagram of Flight Vehicle

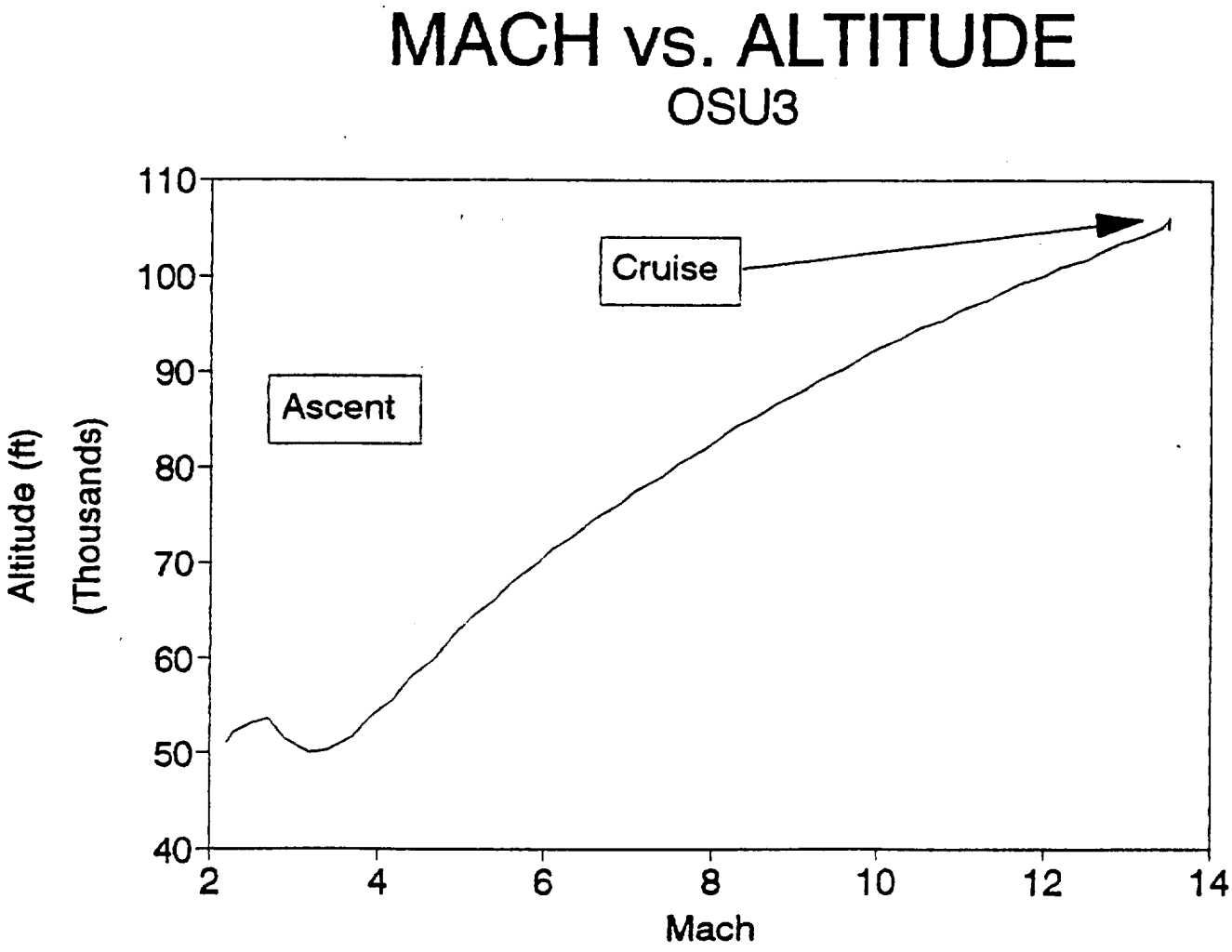
MACH vs. ALTITUDE
OSU3
Altitude (ft)
(Thousands)
110
100
90
80
70
60
50
40
Cruise
Ascent
2
4
6
8
10
12
14
Mach

Figure 9

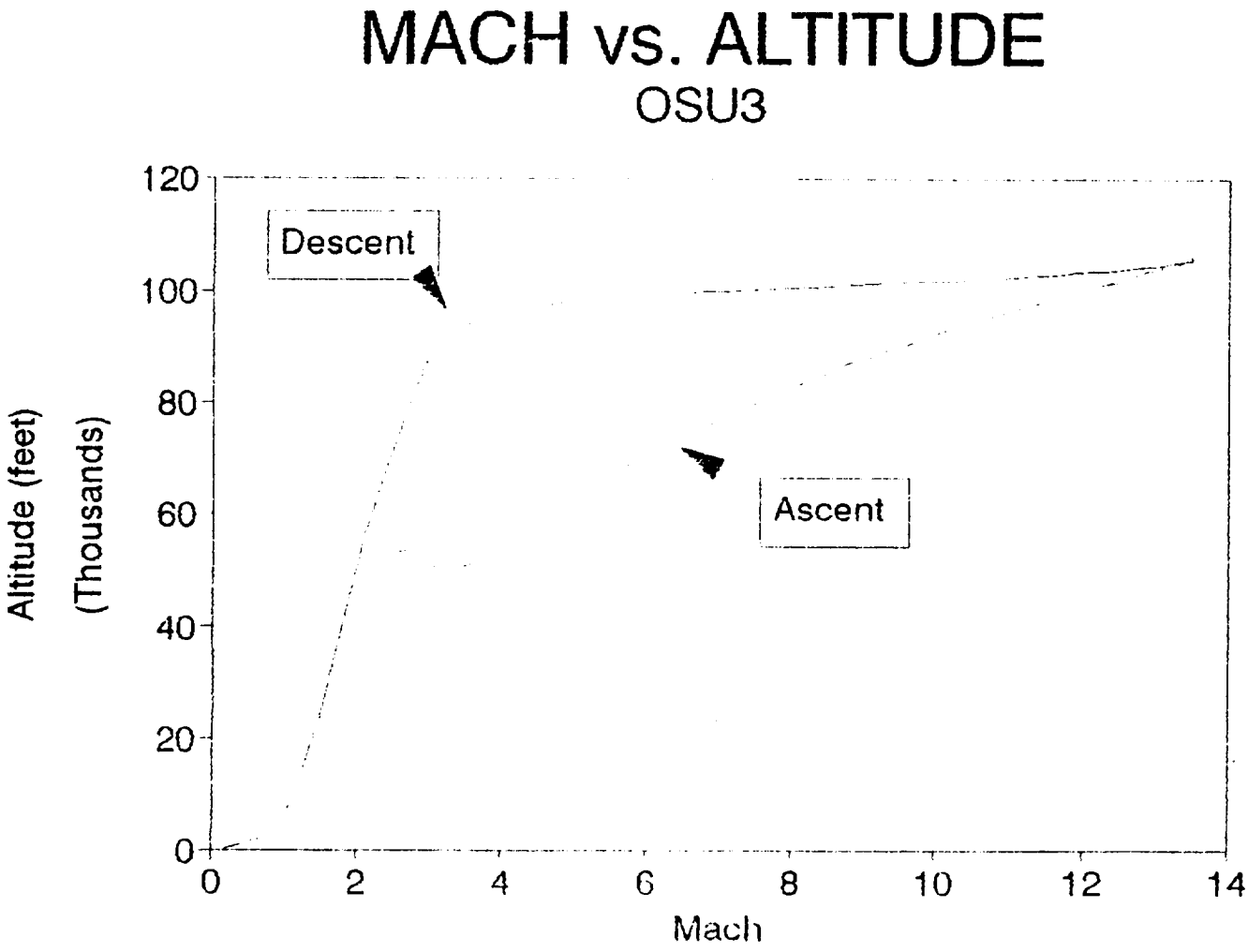
MACH vs. ALTITUDE
OSU3
Altitude (feet)
(Thousands)
120
100
80
60
40
20
0
Descent
Ascent
0
2
4
6
8
10
12
14
Mach

Figure 10

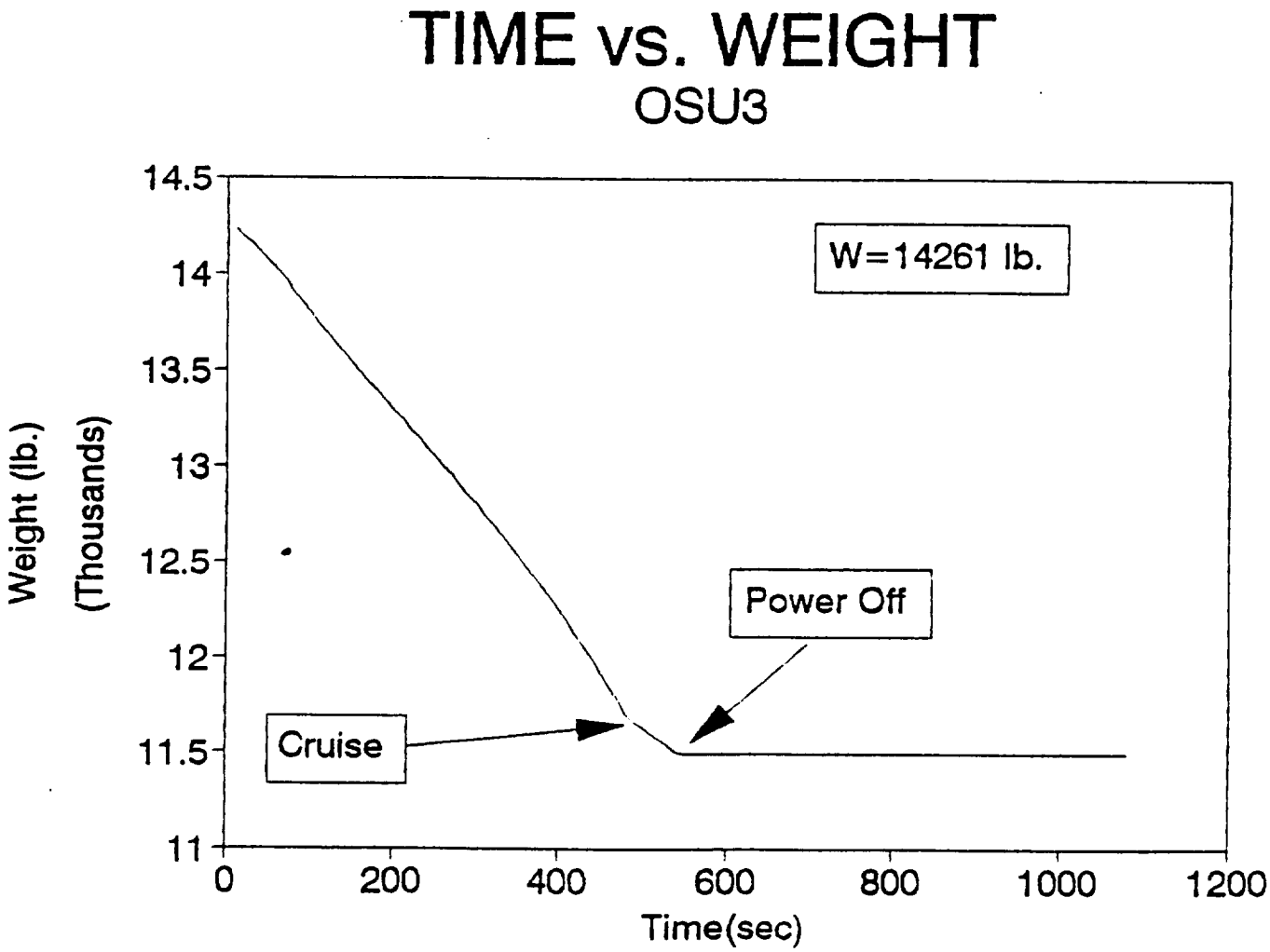
TIME vs. WEIGHT
OSU3
Weight (lb.)
(Thousands)
14.5
14
13.5
13
12.5
12
11.5
11
0
200
400
600
800
1000
1200
Time(sec)
W=14261 lb.
Power Off
Cruise

Figure 11

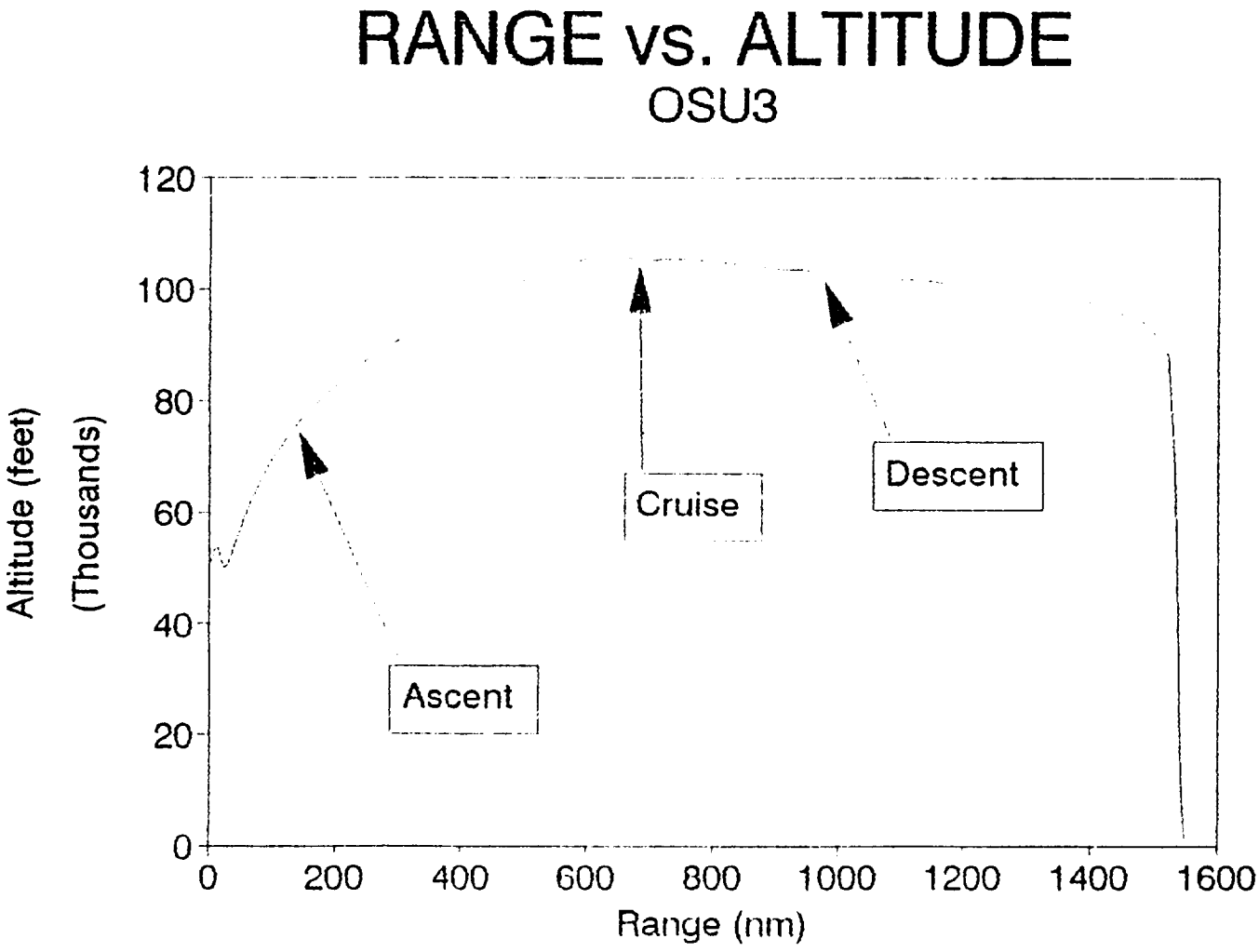
RANGE vs. ALTITUDE
OSU3
Altitude (feet)
(Thousands)
120
100
80
60
40
20
0
0
200
400
600
800
1000
1200
1400
1600
Range (nm)
Ascent
Cruise
Descent

Figure 12

Figure 13

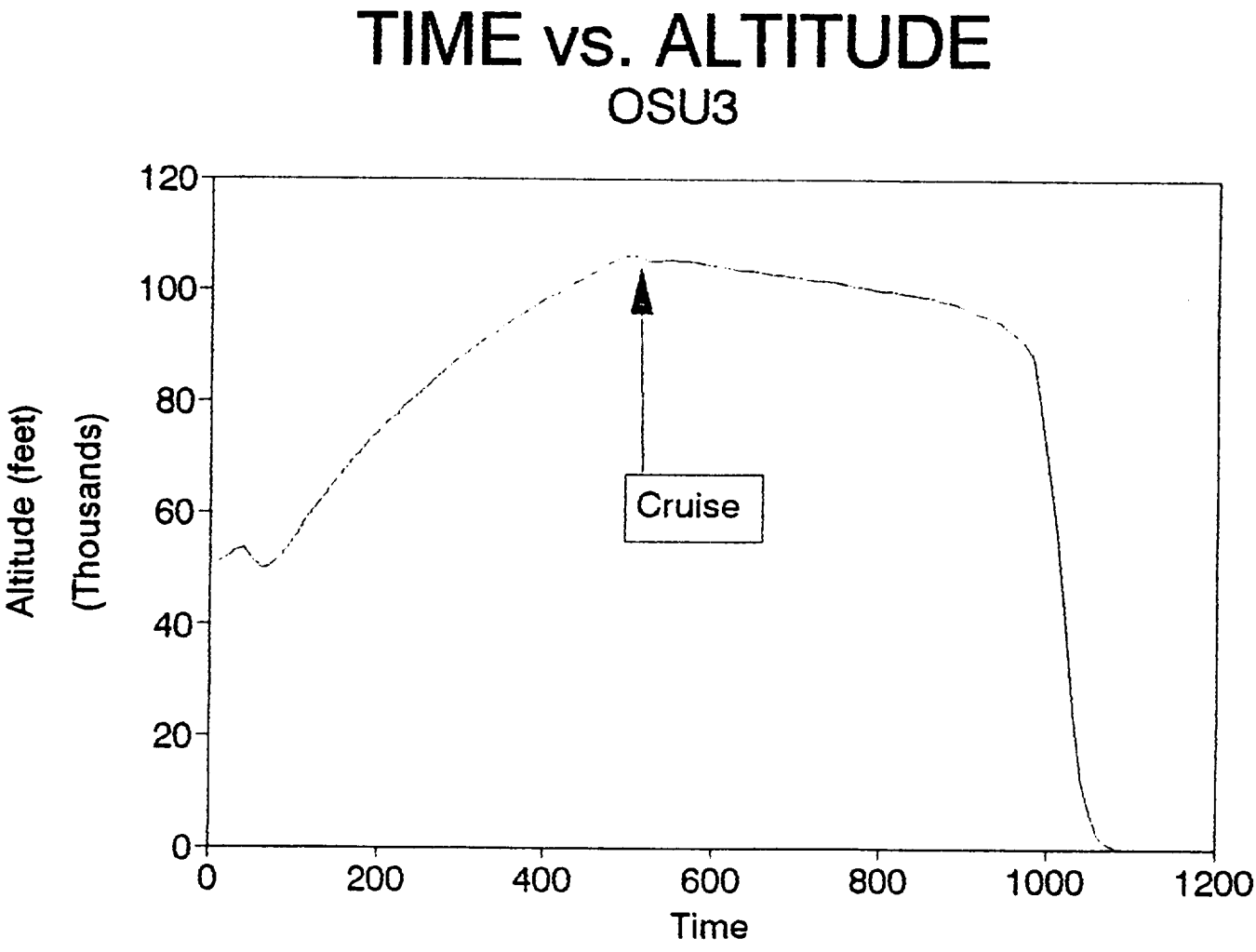

Figure14

PERFORMANCE COMPARISON OF FUELS

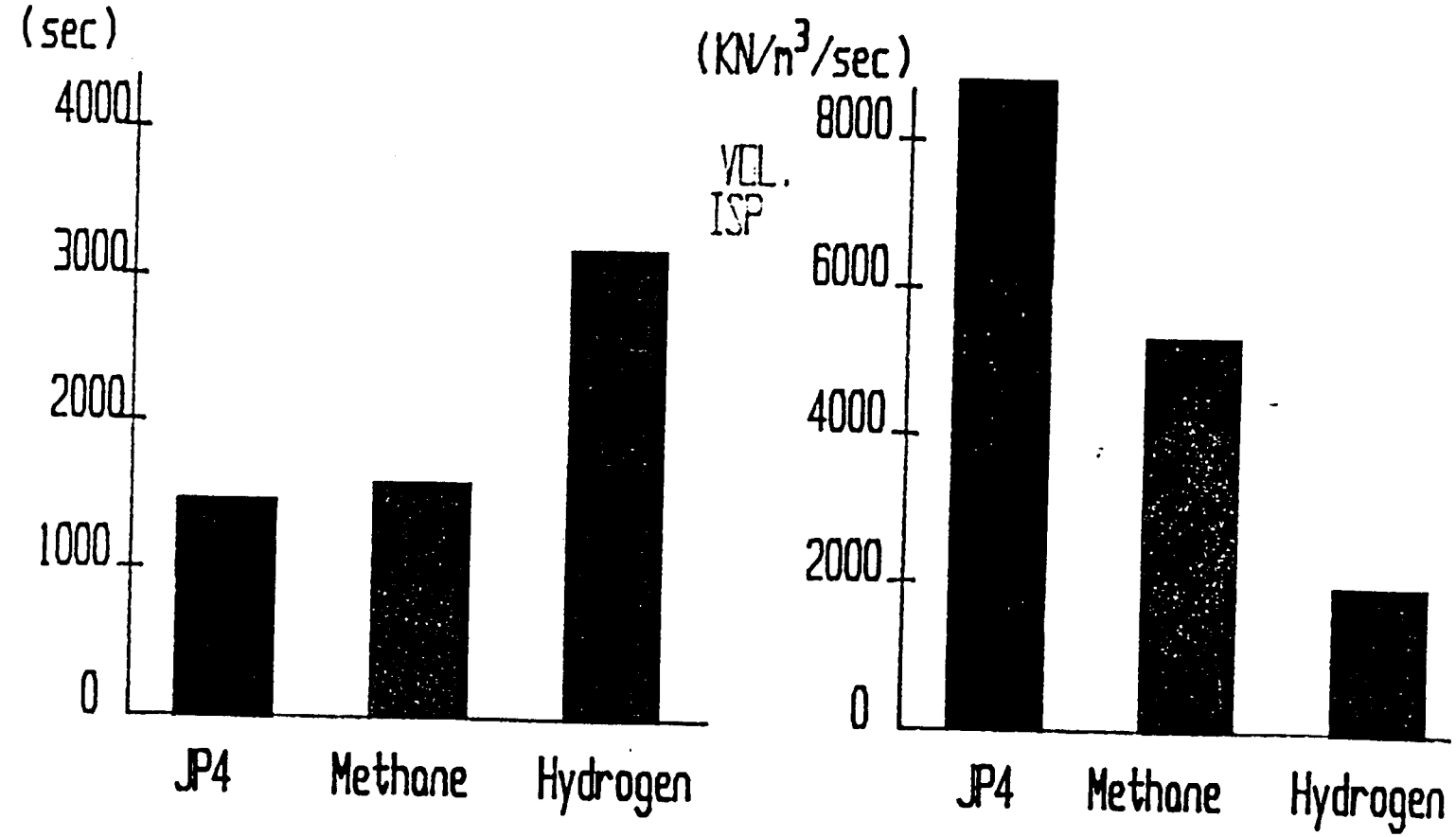

Figure 17

Figure 18

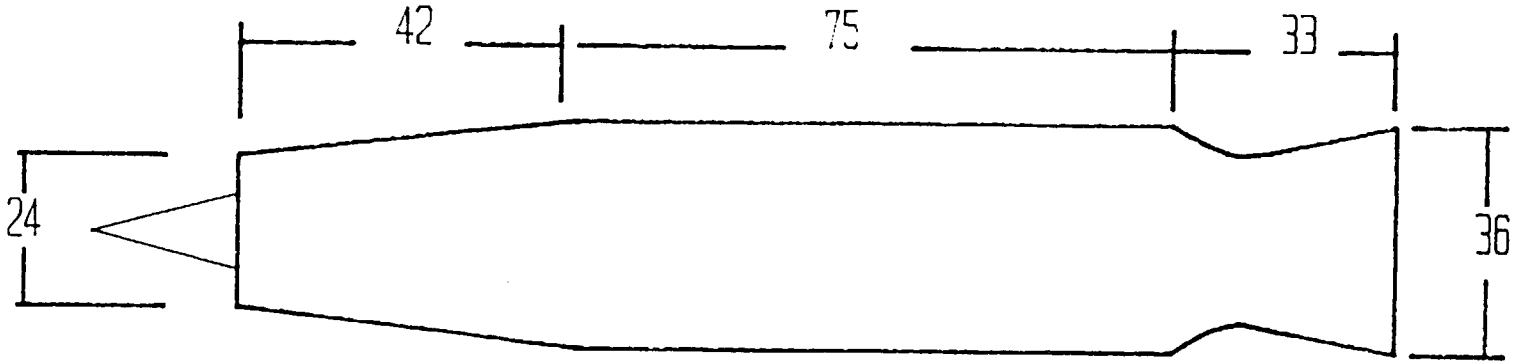

(Dimensions in inches)

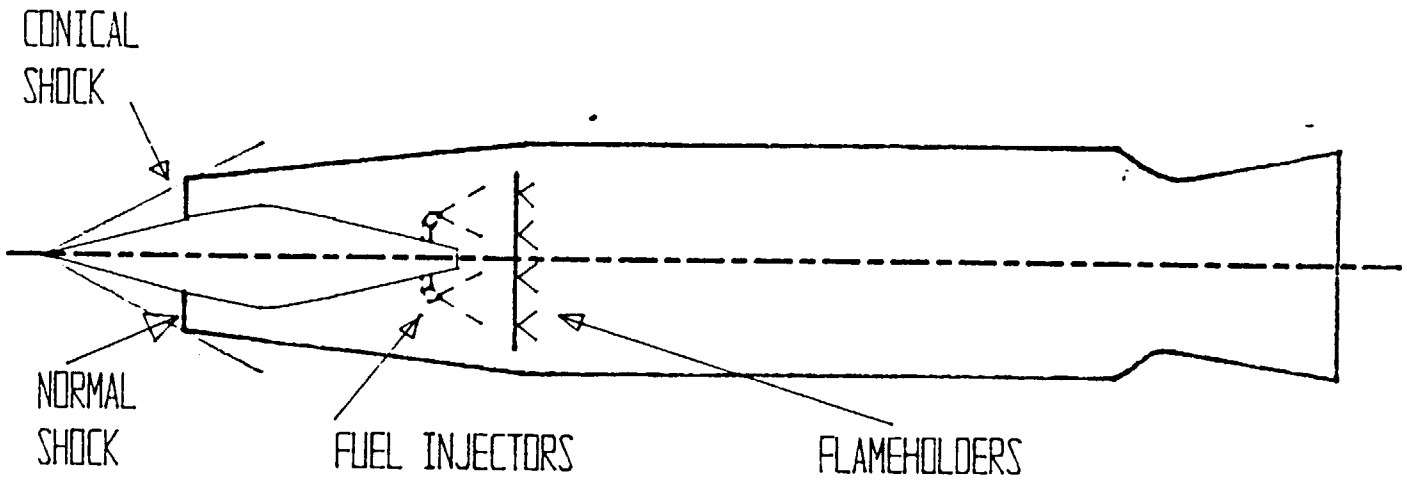

RAMJET ENGINE (Marquardt XRJ59-MA-3)

Figure 19

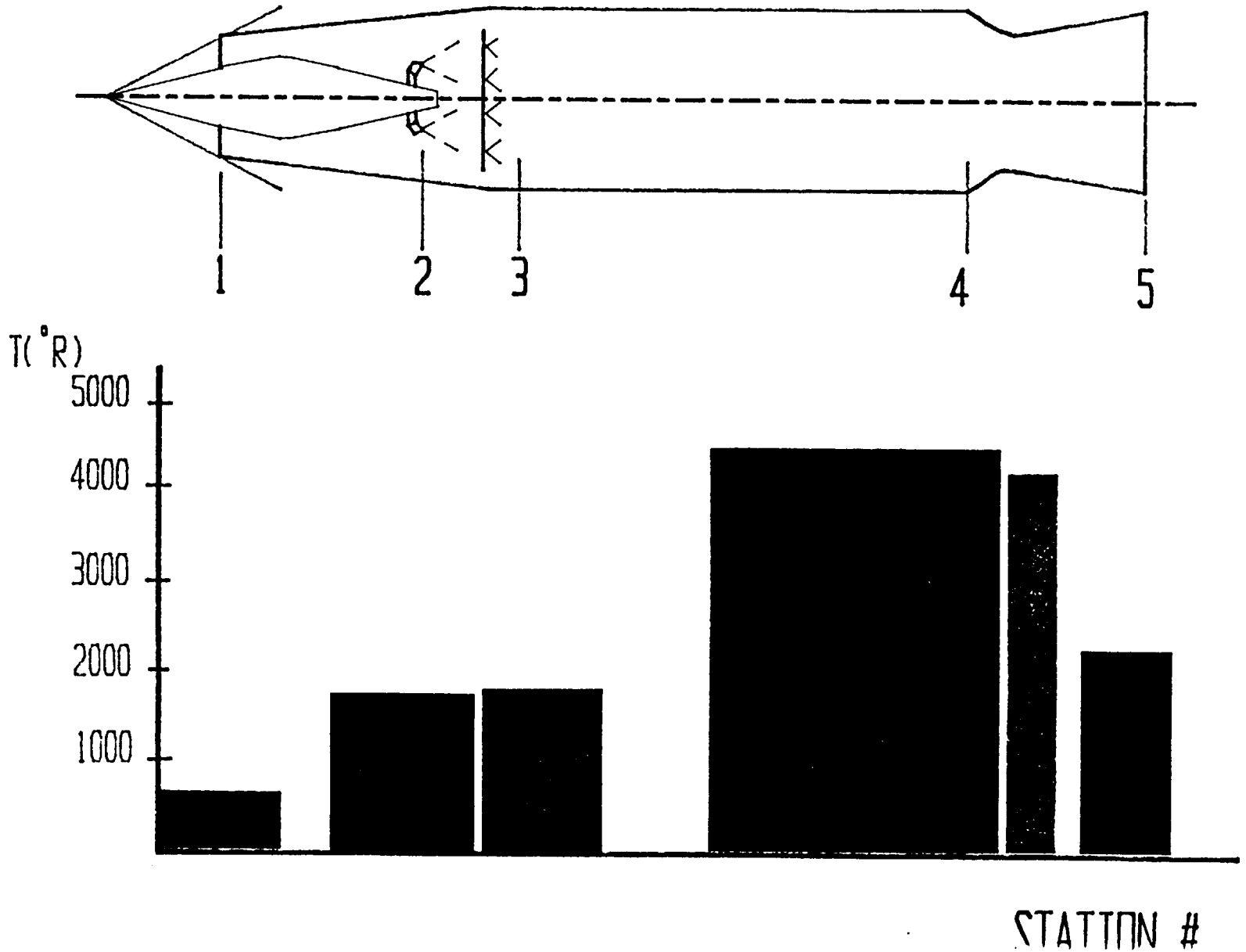

Figure 20

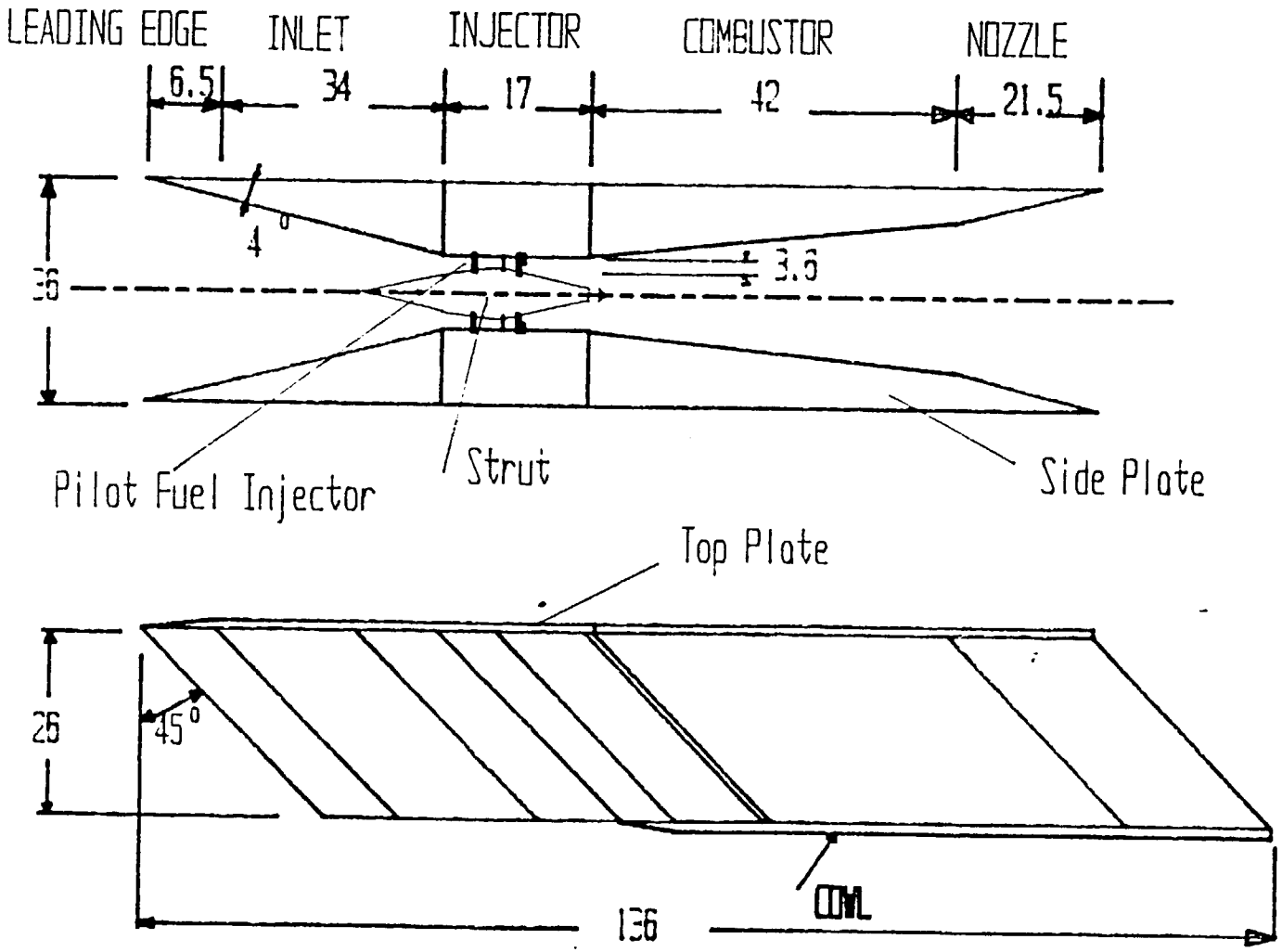

(Dimensions in Inches)

WATER-COOLED SCRAMJET ENGINE

Figure 21

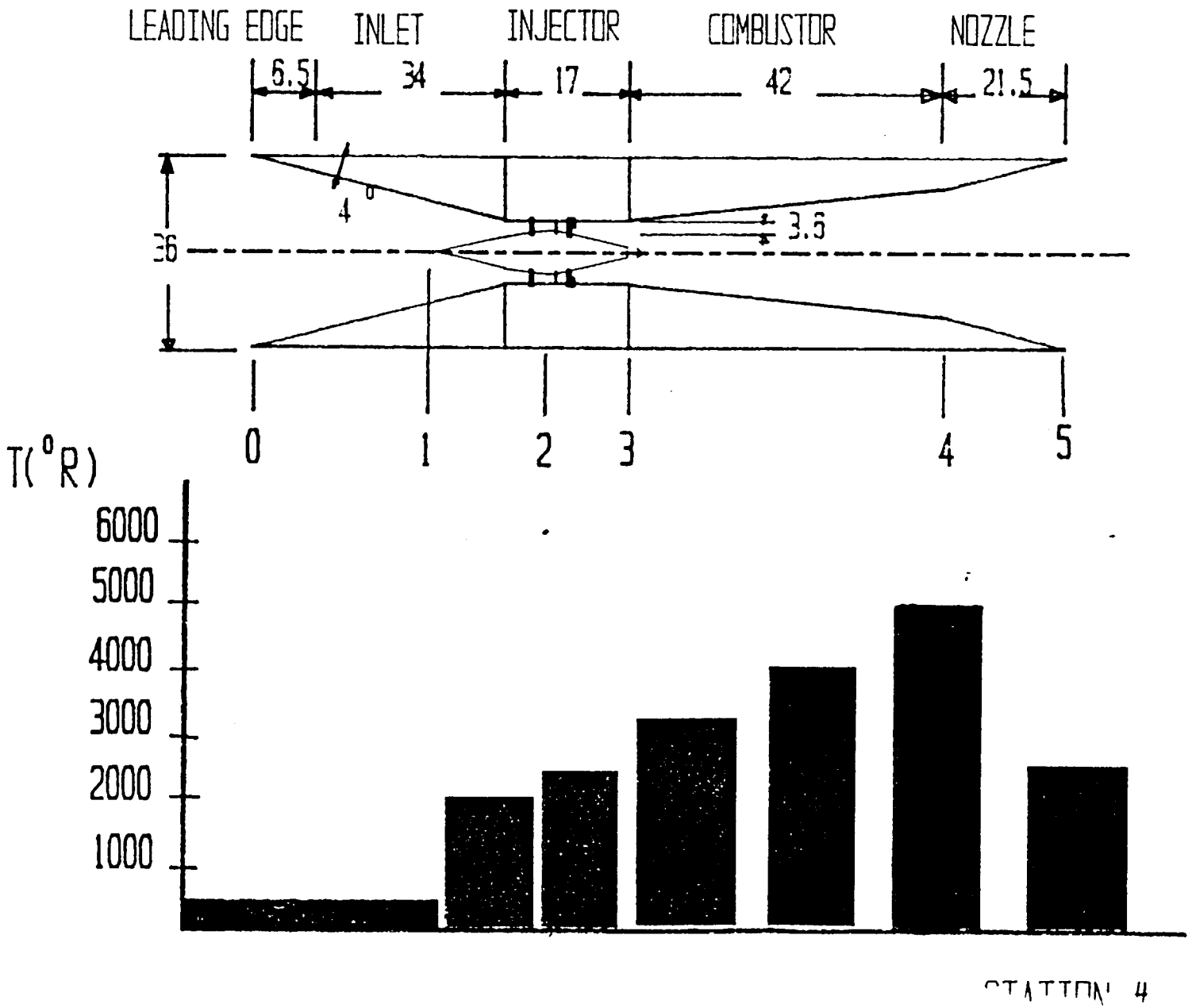
LEADING EDGE
INLET
INJECTOR
COMBUSTOR
NOZZLE
6.5
34
17
42
21.5
4°
3.6
36
0
1
2
3
4
5
T(°R)
6000
5000
4000
3000
2000
1000
STATION 4

OSU III
WEIGHT PIE CHART

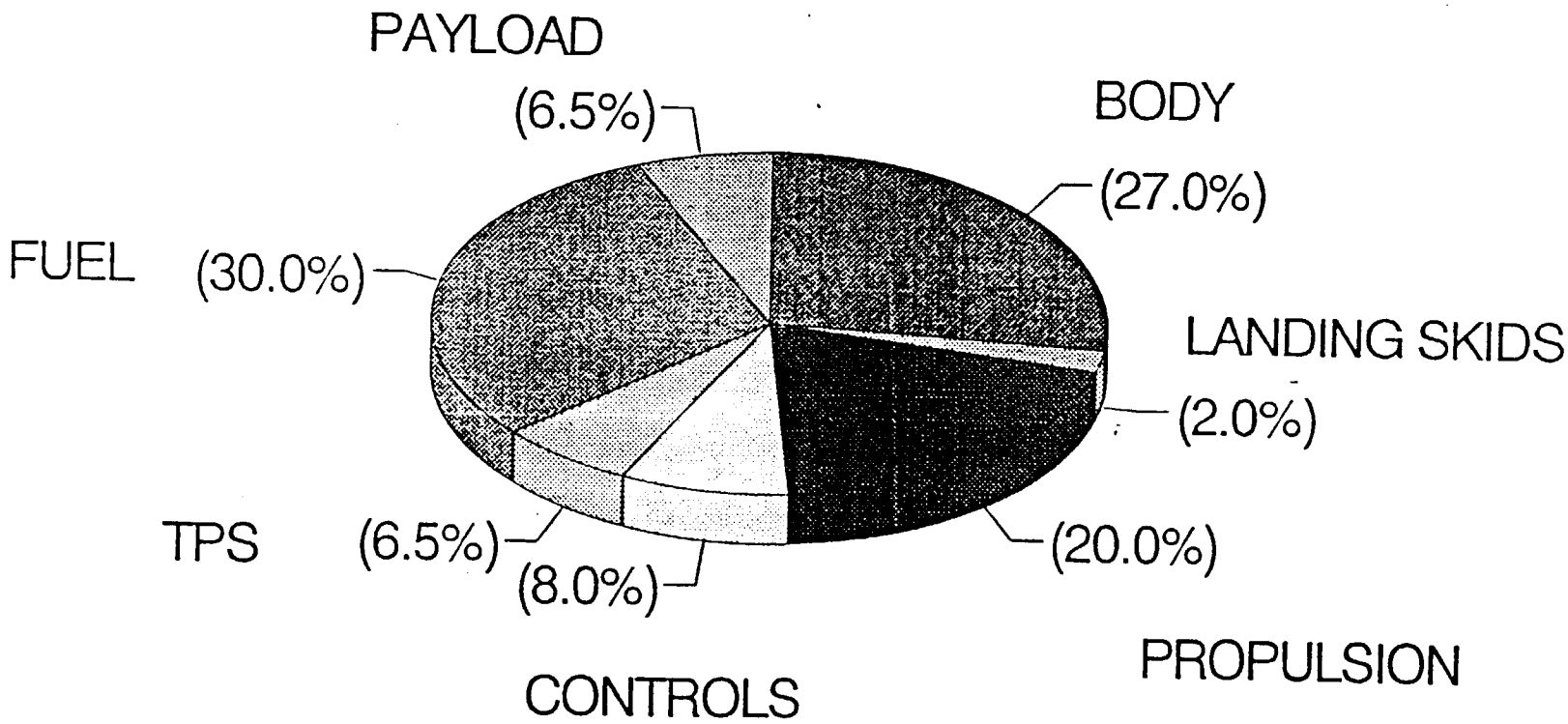

Figure 23

Skid Landing Gear Schematic

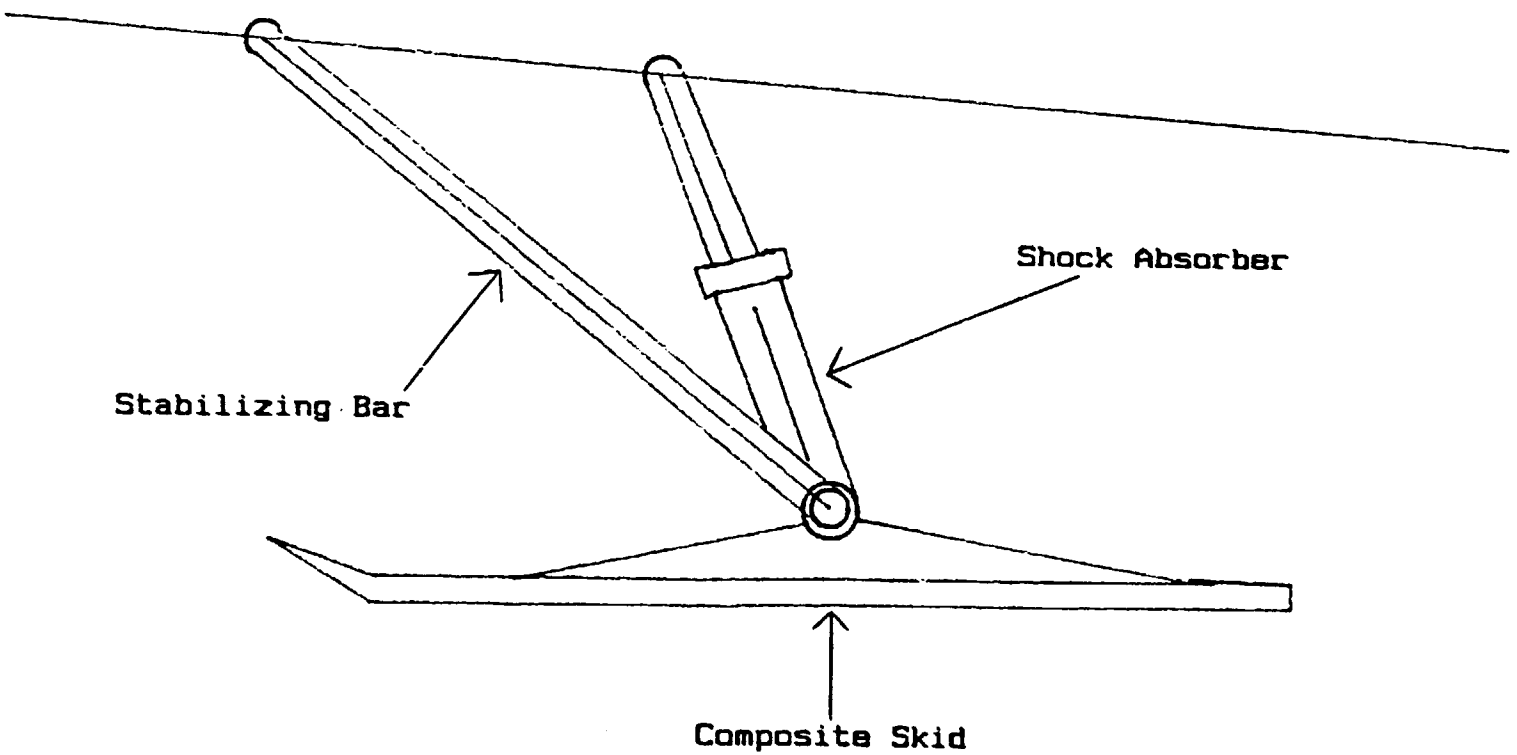

Figure 25

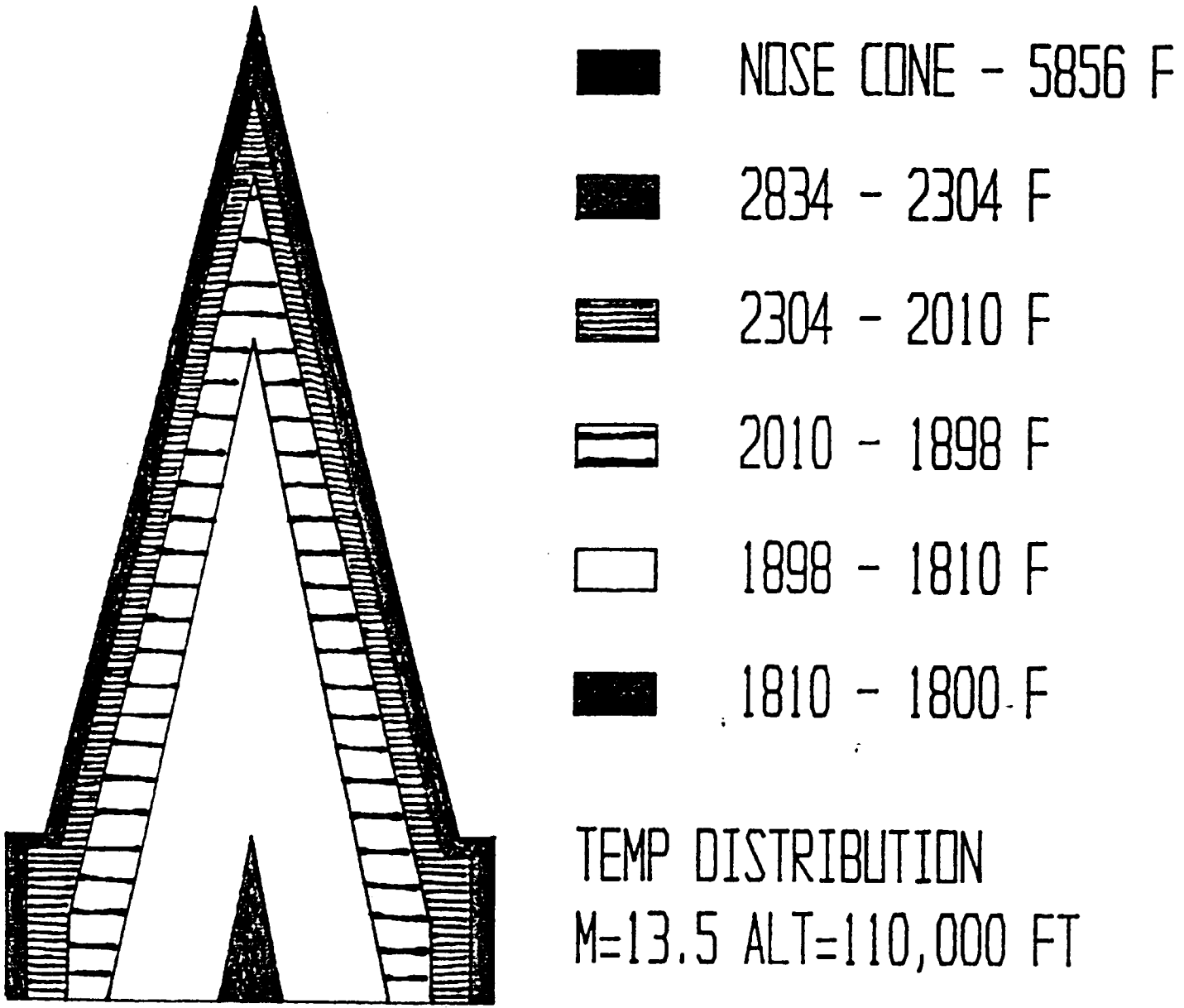
NOSE CONE - 5856 F
2834 - 2304 F
2304 - 2010 F
2010 - 1898 F
1898 - 1810 F
1810 - 1800 F
TEMP DISTRIBUTION
M=13.5 ALT=110,000 FT

Figure 25

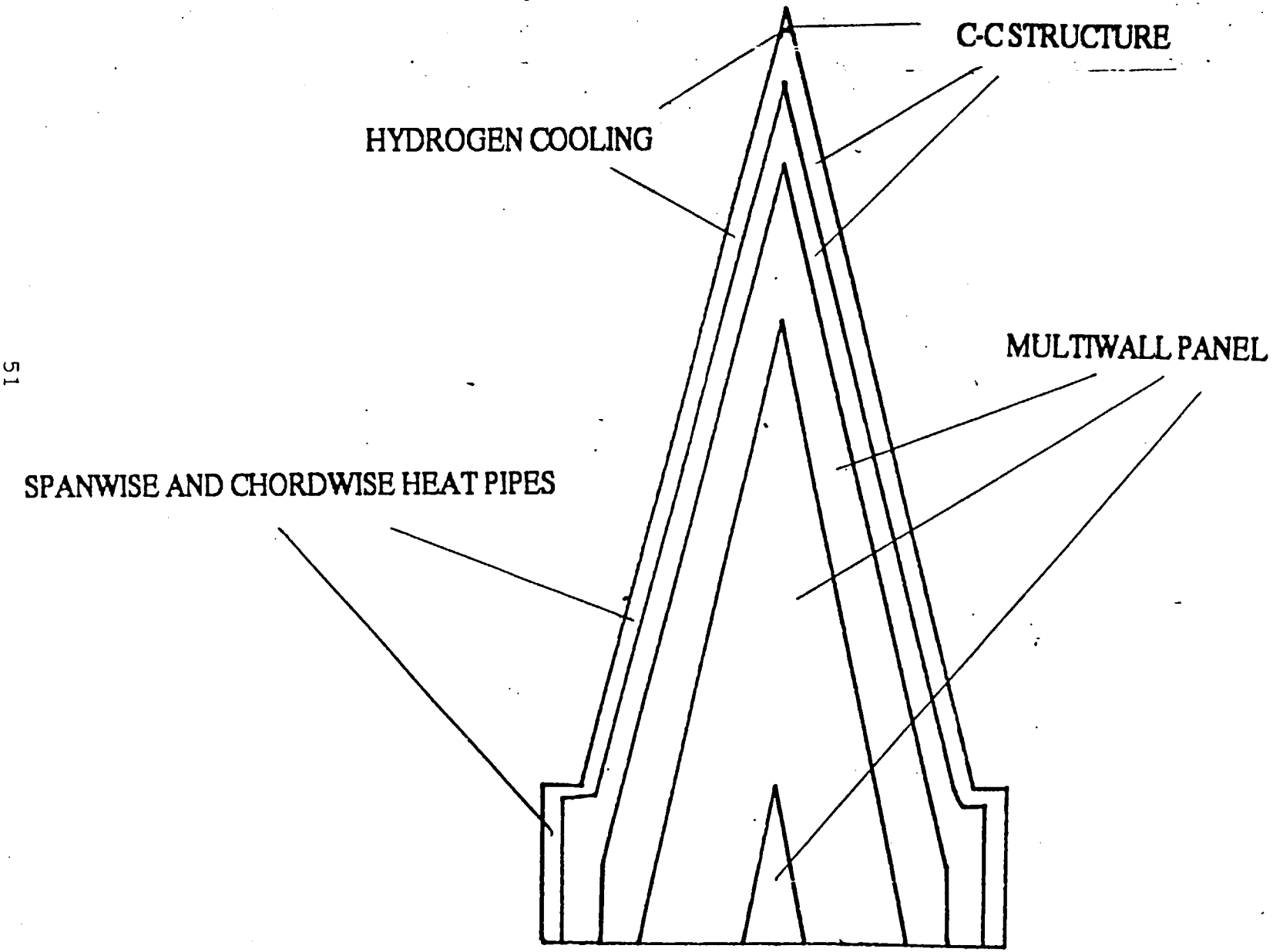
C-C STRUCTURE
HYDROGEN COOLING
MULTIWALL PANEL
SPANWISE AND CHORDWISE HEAT PIPES

Figure 26